

Generation of felsic crust in the Archean: A geodynamic modeling perspective



E. Sizova ^{a,*}, T. Gerya ^{b,c}, K. Stüwe ^a, M. Brown ^d

^a Department of Earth Science, University of Graz, Austria

^b ETH-Zurich, Institute of Geophysics, Switzerland

^c Geology Department, Moscow State University, 119199 Moscow, Russia

^d Department of Geology, University of Maryland, College Park, MD 20742, USA

ARTICLE INFO

Article history:

Received 7 May 2015

Received in revised form

28 September 2015

Accepted 7 October 2015

Available online 19 October 2015

Keywords:

Tonalite-Trondjemite-Granodiorite (TTG)

Continental crust

Archean

Plume tectonics

Subduction

Crustal convection

ABSTRACT

As a consequence of secular cooling of the Earth, there is generally no modern analog to assist in understanding the tectonic style that may have operated in the Archean. Higher mantle temperatures and higher radiogenic heat production in the Archean Earth would have impacted the thickness and composition of the crust. For this reason, well-constrained numerical modeling, based on the fragmentary evidence preserved in the geological record, is the most appropriate tool to evaluate hypotheses of Archean crust formation. The main lithology of Archean gray gneiss complexes is the sodic tonalite-trondjemite-granodiorite (TTG) suite. Melting of hydrated basalt at garnet amphibolite, granulite or eclogite facies conditions is considered to be the dominant process that generated the Archean TTGs. Taking into account geochemical signatures of possible mantle contributions to some TTGs, models proposed for the formation of Archean crust include subduction, melting at the bottom of thickened continental crust and fractional crystallization of mantle-derived melts under water-saturated conditions. We evaluated these hypotheses using a 2D coupled petrological-thermomechanical tectono-magmatic numerical model with initial conditions appropriate to the Eoarchean-Mesoarchean. Based on the result of our experiments, we identify three tectonic processes by which intermediate to felsic melts may be generated from hydrated primitive basaltic crust: (1) delamination and dripping of the lower mafic crust into the mantle; (2) local thickening of the crust; and (3) small-scale crustal overturns. In the context of stagnant-deformable lid tectono-magmatic geodynamic regime that is terminated by short-lived subduction, we identify two distinct types of continental crust. The first type is a pristine granite-greenstone-like crust with dome-and-keel geometry formed over delaminating-upwelling mantle which is mostly subjected to vertical tectonics processes. By contrast, the second type is a reworked (accreted) crust comprising strongly deformed granite-greenstone and subduction-related sequences and subjected to both strong horizontal shortening and vertical tectonics processes. Thus, our study has identified a possible spatial and temporal transition from pristine granite-greenstone-like crust with dome-and-keel geometry to reworked (accreted) crust forming more felsic gneiss terranes in the Archean. We suggest that the contemporaneity of the proposed mechanisms can explain the variety and complexity of the Archean geological record.

© 2015 Elsevier B.V. All rights reserved.

1. Introduction

The greater rate of production of continental crust in the Archean (e.g. Dhuime et al., 2012), and the occurrence of tonalite, trondjemite and granodiorite complexes, and komatiites, which are largely restricted to the Archean (Goodwin, 1991), are

consistent with a hotter Earth. Based on the most primitive liquidus temperatures (Abbott et al., 1994) or mantle potential temperatures (Herzberg et al., 2010) derived by inversion of the chemistry of non-arc basalts from greenstone belts and calculations of the thermal evolution of Earth (Korenaga, 2008a,b; Labrosse and Jaupart, 2007), the upper mantle temperature is estimated to have been up to ~1600 °C in the early Archean. This is ~250 °C higher than the average at the present-day, although the present value varies from 1280 °C to 1400 °C (Herzberg et al., 2007). Higher mantle temperatures together with higher radiogenic heat production, which might have been up to 3 times higher in the Archean (e.g. Brown,

* Corresponding author. Tel.: +43 6601238000.

E-mail addresses: elena.sizova@uni-graz.at (E. Sizova), taras.gerya@erdw.ethz.ch (T. Gerya), mbrown@umd.edu (M. Brown).

2007; Davies, 1992), will have impacted both the thickness and composition of the crust. As a consequence of secular cooling, there is generally no modern analog to assist in understanding the tectonic style that may characterize the Archean, particularly prior to 3 Ga. For this reason, numerical modeling that is constrained by the fragmentary evidence preserved in the geological record is an appropriate tool to evaluate hypotheses of Archean crustal formation.

One of the main lithological associations of Archean gray gneiss complexes is the sodic tonalite–trondhjemite–granodiorite (TTG) suite (Jahn et al., 1981). Since the first description, TTGs have been the subject of much discussion related to their petrogenesis and possible Archean tectonic regimes. Nevertheless, after forty years of investigation there are still many open questions about the generation of TTGs (see overview in Moyen and Martin, 2012). TTGs are a diverse group of silica-rich rocks ($\text{SiO}_2 \approx 64 \text{ wt.\%}$) with high Na_2O contents (3.0 wt.% < Na_2O < 7.0 wt.%) and correlated low $\text{K}_2\text{O}/\text{Na}_2\text{O}$ (0.3–0.6). They contrast sharply with Archean potassio granitoids (Moyen, 2011) and modern granitoids, which are commonly richer in K_2O (granodiorites to granites). One of the crucial points about Archean geology is that the oldest preserved felsic plutonic rocks are mostly TTGs, particularly before 3.2 Ga, while potassio granitoids appear later in Earth history, locally after 3.2 Ga, e.g. in the Barberton area (Kamo and Davis, 1994), and globally by the end of the Archean (Keller and Schoene, 2012). In addition, high-Mg monzodiorites and granodiorites (sanukitoids), which are thought to derive primarily by hybridization between mantle peridotite and a component rich in incompatible elements, occur in many late Archean terrains (Martin et al., 2005). Based on these secular changes in the typology of granitoids, Laurent et al. (2014) proposed a transition to a global plate tectonics geodynamic regime during the late-Archean (3.0–2.5 Ga). This last proposition raises one of the main unanswered questions in understanding the Earth during the Precambrian: what were the tectono-magmatic processes that prevailed in the Archean Eon, particularly during early Archean time, that were responsible for the construction of the unique Archean crust?

1.1. The formation of Archean TTGs

Although the TTGs as a group are diverse with a continuum of compositions, Moyen (2011; see also Moyen and Martin, 2012) has classified them into three types related to the depth of melting in the source: (1) a high pressure group comprising about 20% of TTGs, formed at $P > 1.6$ –1.8 GPa (rutile present) and characterized by higher values of Al_2O_3 , Na_2O and Sr, and lower values of the HREEs (heavy rare earth elements), Nb and Ta; (2) a low pressure group comprising about 20% of TTGs, formed at $P < 1.0$ –1.2 GPa (garnet absent) and characterized by lower values of Al_2O_3 , Na_2O and Sr, and higher values of the HREEs, Nb and Ta; and (3) a medium pressure group comprising about 60% of TTGs, with intermediate geochemical characteristics. According to Moyen and Martin (2012), only high- Al_2O_3 sodic granitoids with low HREEs should be named TTGs. Nevertheless, the term TTG is commonly used for a wide range of sodic plutonic rocks, in some cases even including the associated potassio granitoids.

The main geochemical features of the three types of TTGs relate to the stability of plagioclase, garnet and rutile during melting. The modal proportion of garnet in the residual assemblage in equilibrium with the melts progressively increases from <5% at 1.0 GPa, which results in less pronounced depletion in the HREEs in the low pressure group, up to ~40% at 2.5 GPa, which leads to the pronounced depletion in the HREEs in the high pressure group (Moyen and Martin, 2012; Zhang et al., 2013). The temperature of formation of the low and medium pressure TTG melts varies from 700 °C to 1000 °C, while for high pressure TTG melts the range is from

1000 °C to 1100 °C (Moyen, 2011). Taking into account all of the characteristics of TTGs, there is a growing consensus supporting the generation of TTGs by melting of hydrous metabasalt at garnet amphibolite, granulite or eclogite facies conditions (e.g. Barker and Arth, 1976; Condie, 1986; Foley et al., 2002; Jahn et al., 1981; Martin, 1986; Moyen and Stevens, 2006; Rapp et al., 1991; Springer and Seck, 1997), although alternative models persist as discussed below.

The diversity in the composition of TTGs has led to different tectonic settings being proposed for the formation of the parental melts. Formation within a subduction zone takes into account the necessity to melt hydrated basalts at garnet amphibolite, granulite or eclogite facies conditions and allows for the interaction of TTG melts with mantle peridotites in the mantle wedge (e.g. Arth and Hanson, 1975; Condie, 1981; Hastie et al., 2015; Martin, 1986; Martin and Moyen, 2002). In this model, the high proportion of TTGs in the Archean crust is commonly explained by more extensive slab melting due to higher temperature in the subduction zone (e.g. Moyen and Stevens, 2006). Moyen and Stevens (2004) showed that the low-pressure TTGs appeared earlier in the geological record (around 3.55 Ga), while the high-pressure TTGs occurred somewhat later (3.45–3.22 Ga), which they interpreted as a change from the formation of TTGs in an intra-oceanic continental nucleus to the generation of TTG melts in subduction zones. On the other hand, similar geochemical characteristics to those associated with subduction might be expected from formation of the TTG melts by delamination of the lower crust (e.g. Bédard, 2006). During delamination, sinking blocks of mafic rock might interact with the mantle in a similar way to the interaction between the subducting plate and the overlying mantle wedge (Moyen and Martin, 2012).

Indeed, the main alternative model to subduction for the generation of TTG melts is by partial melting at depth in thickened crust or at the base of oceanic plateaus (Atherton and Petford, 1993; Bédard, 2006; Qian and Hermann, 2013; Smithies, 2000; Zhang et al., 2013). Furthermore, based on melting experiments, Qian and Hermann (2013) and Zhang et al. (2013) argue that it may not even be necessary to over-thicken the crust since the most appropriate conditions for producing low-to-intermediate pressure TTG melts from mafic lower crust are 800–950 °C at 1.0–1.25 GPa, which corresponds approximately to depths of 35–44 km (using a crustal density of 2900 kg/m³). Based on the geochemistry of Archean TTGs and the subcontinental lithospheric mantle (SCLM), Bédard (2006) proposed that TTG melts were derived from the base of thick basaltic plateaus formed above mantle upwellings (plumes in his model, but with higher mantle temperatures in the Archean these upwelling need not be deeply sourced). He argued that delamination of crustal residues after such melting could catalyze multi-stage melting of the SCLM and allow maturation of the Archean continental crust. In a subsequent development, Bédard et al. (2013) proposed a model of cratonic drift in response to mantle wind for the aggregation of Archean cratonic and oceanic terranes (basaltic plateaus), including the development of structures related to bulk regional horizontal contraction. The accretion of terranes led to thickening and delamination of mafic crust coupled with ascent of hot mantle generating voluminous pulses of coeval basalt and TTG magmas.

Lastly, Kleinhanss et al. (2003) proposed an alternative scenario for the formation of TTG melts within the suprasubduction mantle wedge by fractional crystallization under water-saturated conditions. They invoked a major role for aqueous fluid in the formation of Archean TTGs, and further suggested that as the role of aqueous fluids diminished with time, so there was a change from sodic (TTGs) to potassio granitoids during the late Archean (cf. Keller and Schoene, 2012). In a similar approach, based on extensive studies of granitoids from the Kohistan batholith, Jagoutz et al. (2013) proposed hydrous fractionation of subduction related magmas in the lower crust of arcs as model for TTG genesis in the Archean.

1.2. Geodynamic modeling

The remaining challenge in Precambrian geology is to develop a successful paradigm of global geodynamics and lithospheric tectonics for the early Earth, such as the plate tectonics paradigm for contemporary Earth, within which the growing number of observational and analytical data may be integrated. Consequently, the debate about geodynamic settings for formation of TTG melts, which had been centered on field relationships and geochemistry, has now been joined by a series of numerical modeling efforts that are somewhat contrasting in approach.

In an early study, [Van Thienen and Van den Berg \(2004\)](#) argued that a plate tectonics regime was unlikely on a significantly hotter Earth. Using a numerical thermo-chemical mantle convection model, these authors proposed that local crustal overthickening leading to the transformation of basalt to eclogite in the lower crust might trigger a resurfacing event, during which a large segment of crust over 1000 km long sank into the mantle within 2 million years. In this scenario, [Van Thienen and Van den Berg \(2004\)](#) identified two possible settings for partial melting of metabasalt: at the base of the new replacement crust, and in the sinking crustal material itself. These authors proposed that melting in these two settings was mostly responsible for the formation of Archean TTGs, in contrast to some other settings suggested in the literature, such as small-scale delamination of the lower crust, crustal thickening, and melting of a mantle diapir, which, they argued, do not account for the $P-T$ conditions determined for most TTG melts. However, [Van Thienen and Van den Berg \(2004\)](#) admitted that ignoring emplacement of basaltic melts within or under the crust in their model might lead to underestimation of the importance of other mechanisms.

More recently, [Thébaut and Rey \(2013\)](#) used thermo-mechanical numerical experiments to investigate the density-driven sagduction (downwelling) of greenstones and the simultaneous rise of granite domes from the hot and weak basement beneath. They did not concentrate on the formation of the felsic basement, taking it as pre-existing. The results of their numerical experiments are consistent with the existing petrological and isotopic data from long-lived hydrothermal systems associated with steeply inclined greenstone belts, where the fluid was derived from the associated ocean. In a further development, [Rey et al. \(2014\)](#) have proposed that the early continents may have generated intra-lithospheric gravitational stresses large enough to drive lateral spreading of thick continental crust to initiate subduction at the continental edges. Again, the origin of the continents was not discussed.

[Moore and Webb \(2013\)](#) invoked a heat-pipe model for the early Earth similar to that on Jupiter's moon Io. These authors argued that as surface volcanism was fed by localized channels of rising basalt (the heat pipes) so the intervening lithosphere was advected downwards to conserve mass. Heating during sinking would lead to melting of the mafic to ultramafic crust. Thus, felsic volcanics and TTG plutons may have been sourced from the downwards-advection lithosphere. [Moore and Webb \(2013\)](#) further suggest that a rapid decrease in heat-pipe volcanism might have led to initiation of plate tectonics around 3.2 Ga.

In a stagnant-lid tectonic regime the mantle driving forces do not exceed the lithospheric yield strength, resulting in a single, continuous rigid plate overlying the mantle. However, in a mobile-lid tectonic regime the mantle driving forces exceed the yield strength of the brittle lithosphere, causing it to fracture into plates that move relative to each other. Thus, a transition from one regime to the other might be expected with secular cooling. To investigate such a transition models that develop episodic subduction have started to appear in the literature during the last few years (e.g. [Debaille et al., 2013; Moyen and Van Hunen,](#)

[2012; O'Neill et al., 2007a,b; O'Neill and Debaille, 2014; Rey et al., 2014](#)).

Based on paleomagnetic analysis and numerical modeling, [O'Neil et al. \(2007a,b; see also O'Neill et al., 2015\)](#) argued for episodic plate tectonics in the Precambrian, where higher mantle temperatures would result in lower lithospheric stresses, allowing for rapid pulses of subduction interspersed with periods of relative quiescence (cf. [Moresi and Solomatov, 1998](#)). The idea of a dominantly stagnant-lid regime interspersed with short bursts of subduction is supported by some geochemical data (e.g. [Debaille et al., 2013; Griffin et al., 2013](#)). Additionally, thicker crust and lithosphere might have been a serious limitation to the initiation of subduction in the Archean. If true, a different mode of downwelling ([Davies, 1992](#)) or 'sub-lithospheric' subduction ([Van Hunen and van den Berg, 2008](#)) might have characterized early Earth tectonics, although the conversion of basalt to eclogite may significantly relax this limitation at some stage. Nevertheless, frequent slab breakoffs and crustal delamination may have played a more dominant role in the Precambrian ([Van Hunen and van den Berg, 2008](#)). In a complementary study, [Moyen and Van Hunen \(2012\)](#) argued that the late Archean geological record typically suggests short-lived subduction events, much shorter than at the present-day. They argued that magmatism with arc-like geochemistry in the Archean lasted no longer than a few tens of millions of years. Taken together, these modeling results seem to fit with geochemical observations that suggest frequent alternation of arc-style and non-arc-style volcanism on a similarly short time scale (e.g. [Benn and Moyen, 2008](#)).

1.3. Summary of models for the genesis of TTG melts and the aims of the present study

For more than forty years the origin of Archean TTGs and the tectonic settings in which they could have been generated have been controversial topics. Fractional crystallization of basaltic magma was initially thought to be the dominant mechanism by which TTG magmas formed and this model retains some support in the recent literature (e.g. [Arth et al., 1978; Barker and Arth, 1976; Grove et al., 2003; Hastie et al., 2015; Jagoutz et al., 2013; Kleinhanns et al., 2003](#)). However, increasingly models based on partial melting of amphibolite/granulite/eclogite have become preferred (e.g. [Barker and Arth, 1976; Condie, 1986; Foley et al., 2002; Jahn et al., 1981; Moyen, 2011; Moyen and Stevens, 2006; Qian and Hermann, 2013; Rapp et al., 1991, 2003; Springer and Seck, 1997; Zhang et al., 2013](#)). Also, whether the petrogenesis of TTG melts was associated with subduction remains a matter of debate ([Bédard, 2006; Bédard et al., 2013; Foley et al., 2003; Johnson et al., 2014; Martin, 1986; Martin et al., 2014](#)). To reduce the controversy, a new generation of models is required that addresses the genesis of the unique Archean TTG crust by incorporating geochemical, geological, petrological and geophysical data. Here we present a newly developed 2D coupled petrological-thermomechanical tectono-magmatic numerical model with parameters appropriate to early Archean conditions to address such questions. The model includes spontaneous plate generation and movement, partial melting, melt extraction and melt emplacement resulting in crustal growth, radiogenic heat production, eclogitization, and other factors. The experimental results we report here assist our understanding of the dominant geodynamic regime that prevailed in the early Archean and demonstrate a series of possible tectonic scenarios for the formation of continental silicic melts, including TTGs.

2. Description of the numerical model

For this study we used a petrological-thermomechanical numerical model based on the I2VIS code of [Gerya and Yuen](#)

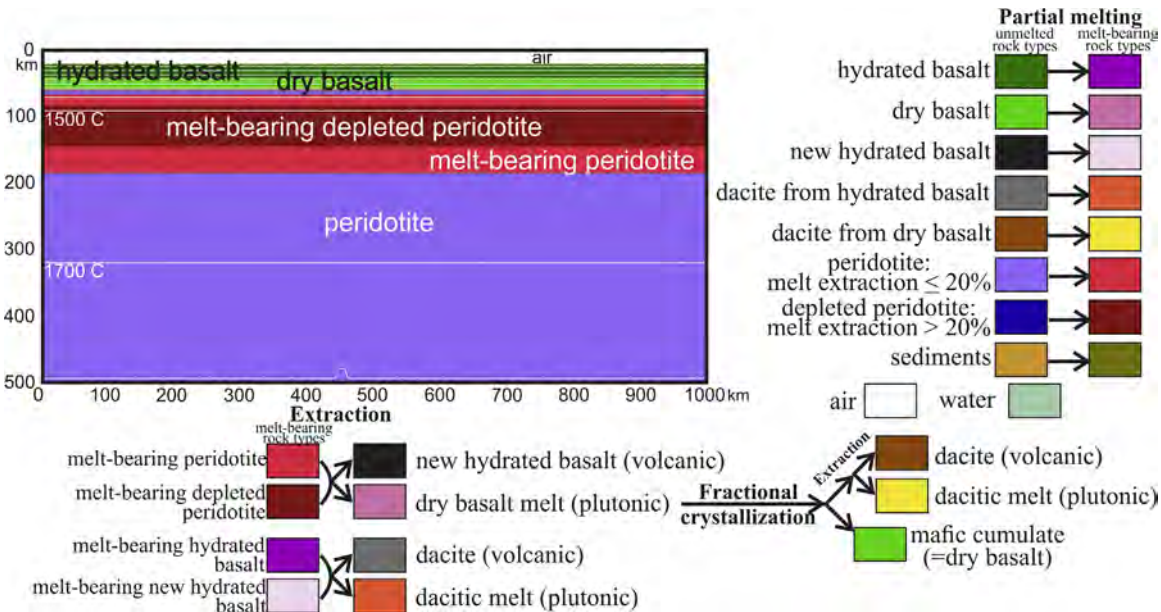


Fig. 1. Initial configuration of the model for the reference experiment (see Section 2.2). White lines are isotherms shown for increments of 200 °C starting from 100 °C. Colors indicate materials (e.g. rock type or melt) which appear in subsequent figures. The interrelations between the materials used for the experiment including partial melting and extraction are shown with arrows. The resolution of the model is 2 km × 2 km. (For interpretation of the references to color in this figure legend, the reader is referred to the web version of this article.)

(2003a). The model describes a series of thermal, chemical and mechanical processes appropriate to a 2D section through the lithosphere and underlying mantle (Fig. 1). The model evolves self-consistently according to the spontaneous material redistribution in response to contrasts in densities and viscosities intrinsic to different lithologies and those induced by temperature variations, partial melting, melt extraction, melt crystallization, mantle depletion, and crustal eclogitization.

The mechanics are described by numerically solving the 2D continuity equation and the conservation of momentum for a compressible visco-plastic medium (Gerya and Yuen, 2007). Temperature evolution is modeled by solving the energy conservation equation with temperature- and pressure-dependent thermal conductivity of rocks as well as adiabatic, radiogenic, latent and shear heat production/consumption. The I2VIS code (Gerya and Yuen, 2003a) used in the modeling combines a conservative finite difference method with a non-diffusive-marker-in-cell technique. A uniform numerical grid resolution of 2 km × 2 km is used for all models. Geological information is included by the use of different properties to represent the various lithologies and melts within the 2D model space, where the lithologies differ in density, rheology and melting properties, and the melts vary from mafic to felsic. The basic details of the numerical model are described in Gerya and Yuen (2003a,b), Sizova et al. (2010, 2014), and Vogt et al. (2012). Compared to these earlier studies, there are differences in the reference model in terms of how we deal with density and melt extraction, and also in the initial and boundary conditions as described below.

2.1. Density and melt extraction

The densities of the various model lithologies are assumed to vary with pressure (P) and temperature (T) according to the equation:

$$\rho_{P,T} = \rho_0 [1 - \alpha(T - T_0)][1 + \beta(P - P_0)], \quad (1)$$

where ρ_0 is the standard density at $P_0 = 1$ MPa and $T_0 = 298$ K, and α and β are the coefficients of thermal expansion and compressibility, respectively. The densities of solid mafic lithologies and of the solid

fraction of partially molten mafic lithologies are adjusted to take into account the increase in density due to eclogitization at depth and the increase in density of the residues due to melt extraction. In the model this is done according to the following amended Eq. (1):

$$\rho_{P,T} = \rho_0 [1 - \alpha(T - T_0)][1 + \beta(P - P_0)] \cdot [1 + \text{coef}_{\text{eccl}} + \text{coef}_{\text{residue}}], \quad (2)$$

where $\text{coef}_{\text{eccl}}$ is a coefficient relating to the degree of eclogitization and $\text{coef}_{\text{residue}}$ is a coefficient relating to the degree of depletion of the source lithology after melt extraction. Based on the experimental data of Ito and Kennedy (2013) for the increase in density due to the conversion of tholeiitic basalt to garnet granulite and eclogite, we implement a linear 0–16% increase in density from the P - T -dependent garnet-in line (the basalt–garnet granulite transition, here implemented at P kbar = 0.014 T°C – 5.4 kbar) to the P - T -dependent plagioclase-out line (the garnet granulite–eclogite transition, here implemented at P kbar = 0.020 T°C + 4.0 kbar). Thus, the $\text{coef}_{\text{eccl}}$ varies from 0 to 0.16 from between these lines. In addition to the $\text{coef}_{\text{eccl}}$ at $P > 10$ kbar, based on the experimental data of Zhang et al. (2013) for the increase in density of garnet-rich residues during progressive melting of amphibolite, we implement a residue coefficient as $\text{coef}_{\text{residue}} = 0.4 M_{\text{ext}}$, where M_{ext} is amount of the melt extracted. Because of the uncertainty and variability of the basaltic source composition for TTG melts in the Archean, we use a single density for basalt in the experiments (present day tholeiitic basalt, 3000 kg/m³). We also consider the density reduction of the mantle beneath the crust due to melt depletion (e.g. Djomani et al., 2001; Griffin et al., 2003). The density of the solid peridotite (and the solid fraction of the partially molten peridotite) is corrected by the coefficient 1–0.04 M_{ext} , which implies a 1% density decrease for the solid residue for every 25 vol.% of melt extraction from the mantle. If the depletion of the peridotite (lilac in Fig. 1) becomes >0.20, then the lithology is changed to depleted peridotite (dark blue in Fig. 1) with the rheology of dry instead of wet olivine (Ranalli, 1995; Table 1). The effective density of all melt-bearing lithologies is calculated from the formula

$$\rho_{\text{eff}} = \rho_{\text{solid}} - M(\rho_{\text{solid}} - \rho_{\text{melt}}), \quad (3)$$

where M is the volumetric fraction of melt present in the rock.

Mantle melting and melt crystallization with $P-T$ are computed according to the parameterized batch melting model of Katz et al. (2003). Melting of crustal rocks occurs in the $P-T$ region between the corresponding solidus and liquidus of the source rock (Table 1). Simplistically, we assume that the degree of both hydrous and dry melting of the crust is a linear function of $P-T$ (e.g. Gerya and Yuen, 2003b). In this model, the volumetric degree of melting, M_0 , is

$$M_0 = \begin{cases} 0 & T < T_{\text{solidus}} \\ \frac{T - T_{\text{solidus}}}{T_{\text{liquidus}} - T_{\text{solidus}}} & T_{\text{solidus}} < T < T_{\text{liquidus}} \\ 1 & T > T_{\text{liquidus}} \end{cases}, \quad (4)$$

where T_{solidus} and T_{liquidus} are, respectively, the solidus T (wet and dry solidi are used for the hydrated and dry rocks, respectively) and dry liquidus T at a given P for a specific lithology (see Table 1). Once the amount of melt, M_0 , for a given marker, is more than zero, the lithology is changed to the melt-bearing analog. Thus, we use the term *melt-bearing* to mean a mixture of solids and liquid as the result of partial melting (or partial crystallization), and *melt* to mean the silicate liquid extracted from melt-bearing rocks.

Although melt might accumulate to some degree in the source, before reaching high melt fractions it is likely to collect in channels and leave the melting zone via dykes (Schmeling, 2006). To simulate melt extraction from partially molten lithologies and partially crystallized melts, several melt extraction thresholds are defined for each material (Table 1; Nikolaeva et al., 2008, p. 341), as follows: M1 – the non-extractable amount of melt that will remain in the source; M2 – the minimum amount of melt that must be present in a melt-bearing lithology for melt extraction to take place; M3 – the maximum amount of melt remaining in a crystallizing melt after which extraction of the fractionated melt may occur (25%, i.e. after 75% crystallization); and, M4 – the maximum value for cumulative melt extraction from a source lithology (i.e. maximum degree of melt depletion).

Markers track the amount of melt extracted during the evolution of each experiment. During melting, the amount of melt (M) available at each marker takes into account the amount of melt previously extracted and is calculated as

$$M = M_0 - \sum_n M_{\text{ext}}, \quad (5)$$

where M_0 is the equilibrium volumetric degree of melting computed at this step as the function of P , T and rock composition and $\sum_n M_{\text{ext}}$ is the total melt fraction extracted during the previous n extraction episodes. If M exceeds M2 but does not exceed M3, the extractable melt fraction $M_{\text{ext}} = M - M_1$ is assumed to migrate upward and the value of M_{ext} is updated. Melt may be extracted until the cumulative total reaches but does not exceed M4. At every time step, extracted melt is transported instantaneously either to the surface as volcanics (20% of M_{ext} , Crisp, 1984) or to a site of plutonic emplacement in the crust (80% of M_{ext} , at sites of highest possible intrusion emplacement rate; see Vogt et al. (2012), p. 4) to form new crust as volcanics at the surface and as intrusions at depth. During a melt extraction episode, the yield strength of a lithology in the column between the source of the melt and the surface is decreased according to λ_{melt} , prescribed as 0.001, which provides significant weakening of the lithologies subject to melt drainage (Sizova et al., 2010, Vogt et al., 2012).

The melt extracted from the mantle that reaches the surface is represented as *hydrated basalt*, due to interaction with sea water when erupted as volcanics at the surface (black in Fig. 1, analogous to the initial hydrated basalt crust, green in Fig. 1; this lithology melts at the wet basalt solidus). In the case of melt emplaced at

Table 1
Properties of the materials used in the experiments (from Bittner and Schmeling, 1995; Poli and Schmidt, 2002; Ranalli, 1995; Schmidt and Poli, 1998; Turcotte and Schubert, 2002). ρ_0 – standard density, k – thermal conductivity, $T_{\text{solidus,liquidus}}$ – solidus and liquidus temperatures of rocks, H_r – radiogenic heat production, M1 – non-extractable amount of melt remaining in the source, M2 – minimum amount of melt required to be present in the rock above which extraction can take place, M3 – the amount of melt remaining in a crystallizing melt after which extraction may occur, M4 – maximum value for cumulative melt extraction from the source.

Material	ρ_0 [kg/m ³] (standard)	Rheology/Flow law	T_{solidus} [K]	T_{liquidus} [K]	H_r [$\mu\text{W}/\text{m}^3$]	M1	M2	M3	M4
Sedimentary and intermediate-felsic rocks	2600 and 2700 correspondingly	Wet quartzite	At $P < 1$ 889 + $\frac{17,900}{(P+54)}$ + $\frac{20,200}{(P+54)^2}$ At $P > 1200$ MPa 831 + 0.06P -/-	1262 + 0.009P	6 and 3 correspondingly	-	-	-	-
Melt-bearing sediments and intermediate-felsic rocks	2400	Wet quartzite	At $P < 1600$ MPa 973 + $\frac{70,400}{(P+354)}$ + $\frac{77,800,000}{(P+354)^2}$ at $P > 1600$ MPa 935 + 0.0035P + 0.0000062P ²	1423 + 0.105P	0.75	-/-	-	-	-
Hydrated basalt/new hydrated basalt	3000	Wet quartzite	At $P < 1600$ MPa 973 + $\frac{70,400}{(P+354)}$ + $\frac{77,800,000}{(P+354)^2}$ at $P > 1600$ MPa 935 + 0.0035P + 0.0000062P ²	1423 + 0.105P	0.75	-/-	-	-	-
Melt-bearing hydrated basalt/new hydrated basalt	2700	Plagioclase An ₇₅	-/-	-/-	0.02	0.04	0.50	0.60	0.60
Dry basalt	3000	Plagioclase An ₇₅	1327 + 0.090P	1423 + 0.105P	0.75	-	-	-	-
Melt bearing dry basalt	2700	Wet/dry olivine	-/-	-/-	0.02	0.04	0.25	0.50	0.50
Peridotite/depleted peridotite	3300	Wet/dry olivine	1394 + 0.133P + 0.0000051P ²	2073 + 0.114P	0.044	-/-	-	-	-
Melt-bearing peridotite/depleted peridotite	2900	Wet/dry olivine	-/-	-/-	0.00	0.05	0.50	0.60	0.60
Reference ^a	1.2	3	4	4	1				

^a 1 – (Turcotte and Schubert, 2002), 2 – (Bittner and Schmeling, 1995), 3 – (Ranalli, 1995), 4 – (Schmidt and Poli, 1998 and Poli and Schmidt, 2002)
-/- – the property is the same as for the previous material.

depth in the crust, it is represented as *dry basalt* (pink when melt and light-green when crystallized in Fig. 1; this lithology melts at the dry basalt solidus). For simplification, all intermediate to felsic lithologies derived from the mafic substrates will be collectively called *dacites* (cf. Vogt et al., 2012). Thus, for example the melts extracted from the melt-bearing hydrated basalt will be called *dacite from hydrated basalt* whether emplaced in the crust or extruded as volcanics on the surface (orange or gray, respectively in Fig. 1).

For the dry basalt melt, which is intrusive into the crust, we apply a low extraction threshold for drainage of fractionated melt after partial crystallization of these melts. Thus, the M3 threshold is prescribed as 0.25, representing 75% crystallization of the dry basalt melt, after which the fractionated more felsic melts may be extracted. These fractionated melts are labeled dacite from dry basalt (yellow in Fig. 1, dark brown if crystallized) when emplaced in the crust or erupted at the surface. We also consider partial melting of the dry basalt (light green in Fig. 1; equivalent to gabbro forming the lower layer of the initial crust or the crystallized intrusive dry basaltic melts subsequently extracted from the mantle). However, we do not separate the melts fractionated from cooling and crystallizing dry basaltic melt and the melts derived from partial melting of dry basalt during heating (melt-bearing dry basalt), and both types of felsic melt are referred to as *dacite*. In this simplified crustal differentiation model, also neglected is any melt extraction from melt-bearing felsic and sedimentary rocks, both of which could produce more K-rich granitic compositions. This additional complexity is not necessary in this study, which concentrates exclusively on the origin of the TTG suite. All melting source and product relationships are shown in the key in Fig. 1.

The *rheological properties* are assumed to follow non-linear viscous and brittle/plastic criteria. We combined the ductile rheology with a brittle/plastic rheology to yield an effective visco-plastic rheology for each lithology. We use the Drucker–Prager yield criterion (Ranalli, 1995), which is implemented by limiting creep viscosity, η_{creep} , as follows

$$\eta_{creep} \leq \frac{\sigma_{yield}}{2\varepsilon_{II}}, \quad (6)$$

where $\sigma_{yield} = c + P \sin(\varphi)$,

$\sin(\varphi) = \sin(\varphi_{solid})\lambda_{melt}$, and

$$\lambda_{melt} = 1 - \frac{P_{melt}}{P_{solid}},$$

Thus, the plastic strength depends on the mean stress on the solids, $P_{solid} = P$ (dynamic pressure), the cohesion, c , which is the strength at $P=0$, and the effective internal friction angle, φ , which is calculated from the friction angle of the solid rocks, φ_{solid} , and the melt pressure factor λ_{melt} . During a melt extraction episode, the yield strength, σ_{yield} , of a lithology in the column between the source of the melt and the surface is decreased according to λ_{melt} . In the numerical experiments we use a low value for λ_{melt} of 0.001, which provides significant weakening of the lithologies subject to melt drainage (Vogt et al., 2012).

2.2. Initial and boundary conditions

To provide a reference for future comparison in experiments with modified parameters, we model crust–mantle interactions in a 1000 km wide and 500 km deep 2D lithosphere–asthenospheric mantle section based on the processes described above and a lithological stratification appropriate to the Archean lithosphere. The initial model configuration is simple (Fig. 1) and assumes the existence of relatively thick primordial mafic crust in the Archean (e.g. Bickle, 1978; Herzberg et al., 2010; Herzberg and Rudnick, 2012;

Johnson et al., 2014; Vlaar et al., 1994). A 40 km thick crust is represented by 20 km of hydrothermally altered basalt (hydrated basalt) on top of 20 km of gabbro (dry basalt). The mantle under this crust consists of peridotite. As part of the initial condition, we assume that 10% of melt had been previously extracted from the upper 300 km of the mantle.

The initial thermal structure of the hotter Archean lithosphere corresponds to a simplified two-stage linear temperature profile defined by 0 °C at the surface, 1200 °C at the crust–mantle boundary (Moho depth, 40 km) and a prescribed 1590 °C on the mantle adiabat at 80 km depth. Thus, the asthenospheric mantle temperature is increased by 250 °C compared to the present-day value. At the lower boundary of the model, the high-temperature boundary condition is prescribed as 2040 °C, but with a small temperature fluctuation to create thermal convective instability during the evolution of the model (Fig. 1). During numerical experiments this initial thermal structure evolves spontaneously toward a more realistic laterally variable geotherm controlled by local crustal thickness and radiogenic heat production as well as mantle heat flow. Radiogenic heat production for all rocks is increased by a factor of 3 (except for the peridotite, which is increased by a factor of 2 to avoid mantle overheating) to satisfy the Eoarchean–Mesoarchean conditions (e.g. Brown, 2007, 2014; Davies, 1992). One consequence of the initial thermal structure is the generation of melt in the upper mantle during the first several thousand years. In the model this melt was removed from further consideration so that the full initial depletion of the upper mantle corresponds approximately to the degree expected after extraction of the prescribed 40 km thick initial mafic crust.

All mechanical boundary conditions are free-slip. The top surface of the lithosphere is treated as an internal free surface by using a 20 km thick top sticky air layer with low viscosity (10^{18} Pa s) and density (1 kg/m³). When the surface sinks below the sea level (20 km) it is covered by water (viscosity 10^{18} Pa s, density 1000 kg/m³). The large viscosity contrast caused by these low viscosity boundary layers minimizes shear stresses (<10⁴ Pa) at the top of the lithosphere making it an efficient free surface (cf. Schmeling et al., 2008). This upper boundary evolves by erosion and sedimentation, as described in detail by Nikolaeva et al. (2008). Because of uncertainty about the H₂O content for Archean lithologies, we neglect H₂O release, transport, and consumption in our experiments.

3. Experimental results

Next we present a detailed description of the reference experiment (Sections 3.1–3.4). In Section 3.5, we summarize the differences between this experiment and other experiments we ran with modified parameters to test the robustness of our results from the reference experiment.

3.1. Model evolution

Fig. 2 shows several stages in the development of the reference experiment during ca. 200 Ma of model time (a complementary animation of the model evolution is provided in *Supplementary material, Movie 1*). Since we do not implement any lateral lithological variations in the initial set-up (only a small temperature fluctuation, see Fig. 1), it takes a few million years in the model for mantle convection to develop and for related gravitational redistribution of materials to begin in the crust and mantle (Fig. 2a,b). During this period the system is cooling down. As a result, the initial melt-bearing peridotite at the top crystallizes forming a relatively thin layer (10–30 km) of sub-crustal mantle lithosphere.

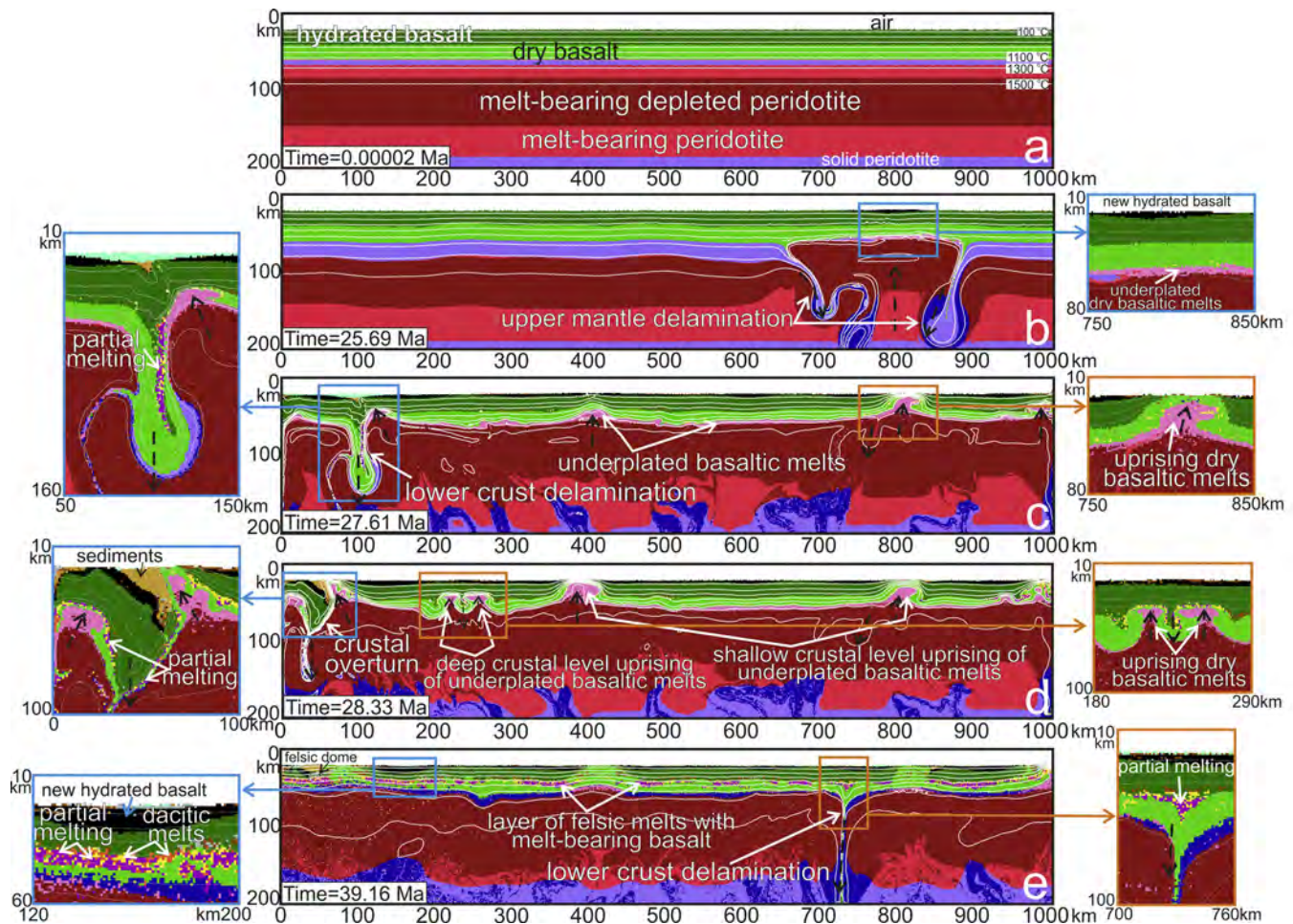


Fig. 2. Representative time-slice snapshots to show various stages during the evolution of the reference experiment (upper-mantle temperature 250 °C higher than the present-day value). Blue and orange frames are supplemented by detailed views of these areas. During the first few million years the system is cooling down, and, as a result, the melt-bearing peridotite crystallizes at the top (a,b). After c. 25 Myrs, simultaneous upwelling of the asthenospheric mantle and delamination of the mantle lithosphere and part of the lower portion of the overlying mafic crust begins at the right-hand side (b,c). Asthenospheric mantle upwellings lead to dry basaltic magmas underplating the lower crust (pink) and the formation of new hydrated basaltic lavas atop the crust (black) (b,c). Rising dry basaltic melts may lead to crustal overturn (blue frame on the snapshot d) or lower crustal delamination (orange frame on snapshot d), and may cause partial melting of the hydrated basalt (violet). Felsic melts extracted from the melt-bearing hydrated basalt (orange) or generated by the fractional crystallization of dry basaltic melts (yellow) mix with the melt-bearing basalt and localize at the bottom of the basaltic crust (e); these melts begin to form domes within the overlying mafic crust (f–g). After c. 69 Ma, multiple large mantle upwellings occur at the left-hand boundary (f–m). The new oceanic plate with a thick basaltic crust on top generated by these upwellings moves to the right causing shortening of the continental-like crust enriched in felsic material and vigorous remelting of a lower crustal layer (g,h). A felsic diapir rising at the contact of the plates leads to a spontaneous oceanic plate subduction (h–o) interrupting by slab breakoff (k,n), and alternating with periods of a dripping regime (i,l). After the second episode of subduction, the trench starts to retreat creating a backarc basin (o). (For interpretation of the references to color in this figure legend, the reader is referred to the web version of this article.)

This embryonic mantle lithosphere is colder and less depleted than the underlying melt-bearing asthenospheric mantle (as defined by the initial conditions); thus it is negatively buoyant. After approximately 25 Ma, a small temperature fluctuation in the upper-mantle on the right-hand side of the model box triggers simultaneous upwelling of the asthenospheric mantle and delamination of the mantle lithosphere together with part of the lower (eclogitized) portion of the original mafic crust (Fig. 2b).

The dripping of the cold dense material provokes the formation of several mantle upwelling zones where the rising hotter, melt-bearing peridotite undergoes additional decompression melting. This leads to basaltic magmas underplating the lower crust (pink in Fig. 2b,c) and the formation of new hydrated basaltic lavas atop the crust (black in Fig. 2b,c). As a consequence of this material redistribution, the most depleted melt-bearing peridotite now appears directly below the crust (e.g. Fig. 2b,c). Cooling and solidification of this highly depleted peridotite together with the transition of the lower mafic crust to eclogite provokes new crust–mantle delamination events that lead to new hot mantle upwelling zones (Fig. 2c,d). These Rayleigh-Taylor type dripping/

delamination instabilities continue throughout almost the entire experiment (ca. 200 Ma).

As the dry basaltic melts locally underplate the crust and accumulate, they are able to rise upwards in a diapiric manner through the overlying mafic crust at sites that had been previously weakened by the upward percolation of basaltic melts now forming the new volcanic sequences atop the original crust (orange frame in Fig. 2c). This episodic crustal convection/diapirism process is commonly spatially associated with (partially molten) eclogite drips from the lower crust (blue frame in Fig. 2c). The strong increase in density of the colder downwelling crust triggering these drips is due to both eclogitization of the lower basaltic crust and extraction of dacitic melt from this crust during partial melting, which increases the amount of garnet in the residue (Eq. (2)).

Crustal diapirism may also trigger crustal overturn events whereby a block of crust including the hydrated basalt from the surface is overturned and comes into contact with the underlying hot melt-bearing peridotite at a depth of 30–60 km (blue frame in Fig. 2d). This sinking crust undergoes partial melting, producing dacite (orange in Fig. 2, or gray when crystallized) that forms

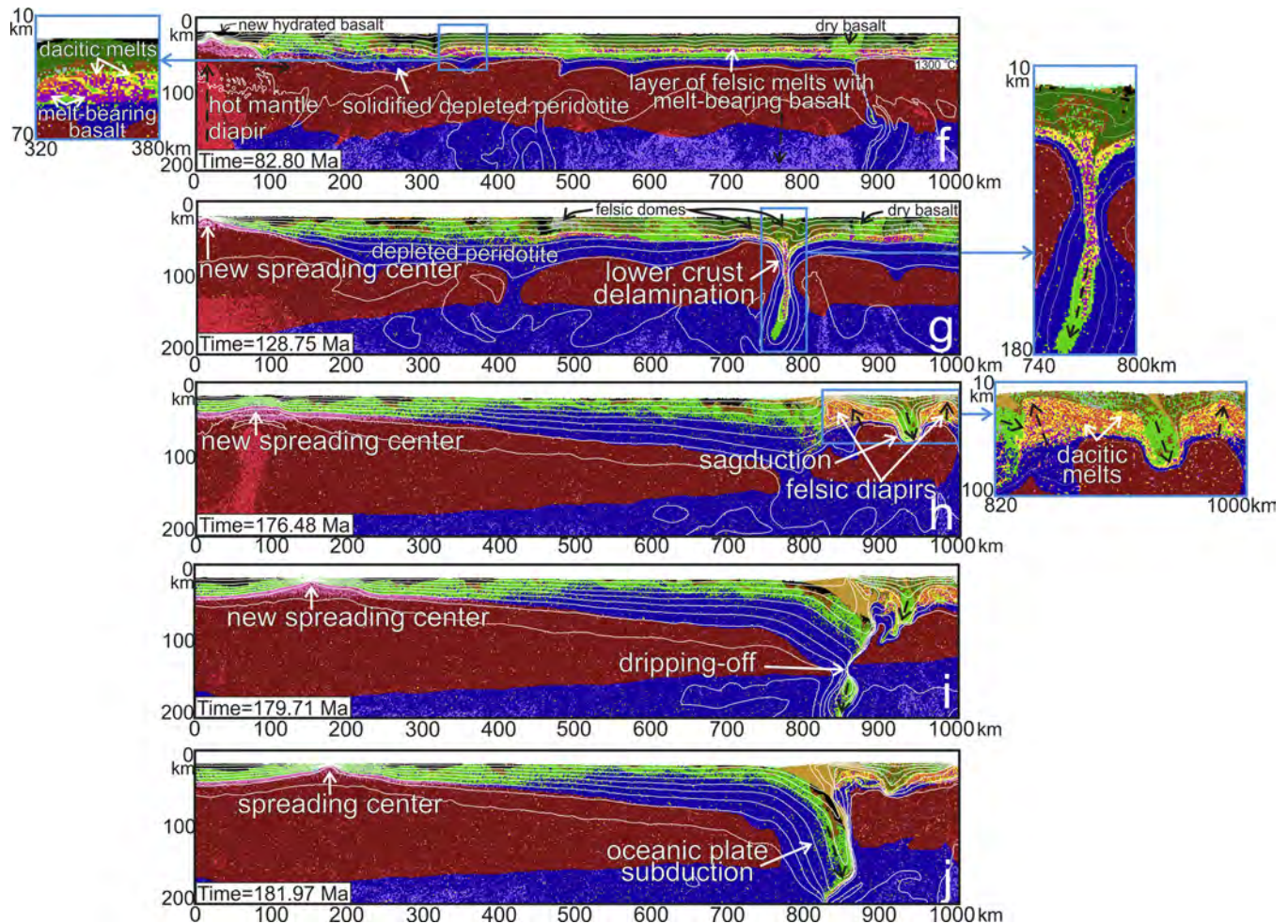


Fig. 2. (Continued)

new felsic continental crust in the experiment. Laterally, where the mafic crust has become thickened both the buried hydrated basalt and the underlying gabbro (dry basalt) in the lower part undergo partial melting to produce dacite (orange and yellow in Fig. 2e, respectively).

In addition, fractional crystallization of the underplated dry basaltic melts produces intermediate-felsic melts (generically called dacite) that may be segregated from the cumulate after 75% crystallization, as specified in the parameters for melt extraction. Over the period of the experiment the dacitic melts generated by fractional crystallization of the dry basaltic melts (yellow) mix with the melt-bearing basalt (violet) and the dacitic melts (orange) generated from it by melting. These hybrid melts form a predominantly felsic layer at the bottom of the basaltic crust (blue frames in Fig. 2e,f). Throughout the period of the experiment the low density and viscosity of this layer, together with additional dacitic melts derived from the hydrated basalt, allows domes to form within the overlying mafic crust, giving rise to the archetypal dome-and-keel structure found in Archean cratons.

On timescales of tens to hundreds of millions of years, these variable tectono-magmatic processes gradually rework the primordial mafic crust into more felsic continental-like crust (cf. Fig. 2a,b and f), composed of alternating basaltic and dacitic domains. Further details of these various tectonic settings in which continental-like crust may be produced are discussed in Section 3.2.

From about 69 Ma, multiple large mantle upwellings occur at the left-hand side of the model (Fig. 2f-h), creating a series of spreading centers that generate new thick basaltic crust (20–40 km)

underlain by depleted mantle peridotite. Over time this process creates a plate of oceanic-type lithosphere (Fig. 2g,h). The plate moves to the right as a result of the upwelling mantle and causes shortening of the continental-like crust enriched in dacitic material. This shortening leads to delamination and dripping of the eclogitic mafic lower crust together with part of the felsic melt-bearing layer (blue frame in Fig. 2g). The rest of the thinned lower crust on either side of the drip undergoes heating by upwelling asthenospheric mantle following the initiation of delamination, thus creating additional felsic melts and also remelting the crystallized felsic layer. In turn, this provokes the ascent of felsic domes within the mafic substrate according to the local compressional and tensional environment, forming lithospheric blocks with dome-and-keel structure that are divided from each other by intrusions of dry basalt (e.g. the right-half of Fig. 2g). Eventually the continental-like crust thickens as the continental-type plate is shortened to <200 km width by about 170 Ma. The elevated geotherms enable vigorous remelting of a lower crustal layer composed mostly of dacites. This felsic layer also forms diapirs triggering downwelling (sagduction) of the overlying mafic crust, mostly comprising intrusions of dry basalt (e.g. blue frame in Fig. 2h; cf. François et al., 2014).

Around 177 Ma a large felsic diapir rises directly at the contact of the oceanic-type and continental-type plates (blue frame in Fig. 2h). This creates a weak zone along which the oceanic-type plate spontaneously subducts to the right beneath the continental-type plate generating surface topography, which allows for erosion and sedimentation triggering formation of an accretionary sedimentary

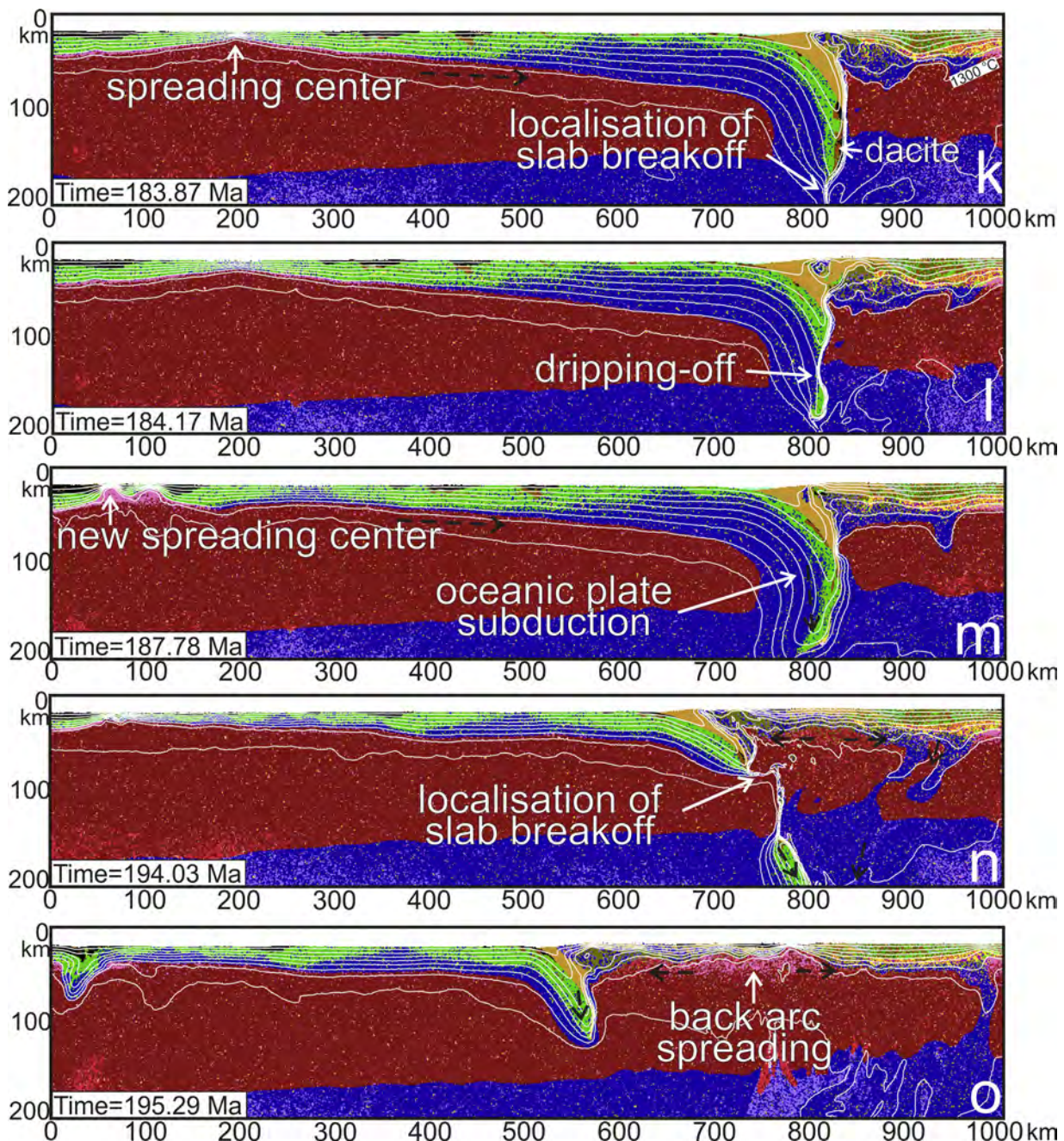


Fig. 2. (Continued)

complex in the trench (Fig. 2h,i). After the short subduction event (up to ~100 km depth), the slab simply hangs in the mantle. During this period the plate tip undergoes heating from the hot surrounding mantle and ultimately drips off (Fig. 2i). The system remains essentially static for c. 3 Ma. Then, as the newly formed spreading center on the left creates an additional push of the oceanic-type plate to the right, subduction resumes (Fig. 2j). This episode of subduction is maintained by the transition of the thick basaltic crust in the subducting plate to eclogite. However, as soon as the part of the oceanic-type plate with a high proportion of dacite becomes involved in the subduction, the slab pull acting on the shallow part of the plate is decreased, which leads to slab stretching and ultimately a breakoff (Fig. 2k). The sedimentary rocks and the new hydrated basalt from the oceanic-type plate are subducted to a maximum of ~100 km depth where they are exposed to conductive

heating from the surrounding hot mantle, which leads to partial melting and subsequent exhumation toward the surface (Fig. 2k,l). After the slab breakoff, the experiment reverts to a crustal lithosphere dripping mode (Fig. 2l). As the next deep mantle upwelling and respective spreading center appears on the left, subduction resumes again (Fig. 2m), and once again this event is terminated by slab breakoff (Fig. 2n). The localization of the slab breakoff in this case occurs at the former spreading center, which has thin and young mantle lithosphere with thinned mafic crust and cannot support the slab pull. From the time of the second subduction event the trench starts to retreat. The retreat causes the rise of melt-bearing hot mantle, thinning of the continental crust, and finally development of a backarc basin (Fig. 2n,o). The previously thickened continental crust is thinned during this stage, from ~50 km to ~30 km on average.

3.2. Geodynamic settings for the formation of continental crust

Melting of hydrated basalt at garnet-amphibolite, granulite or eclogite facies conditions is widely considered to be the dominant process for the generation of TTG melts in the Archean (e.g. Barker and Arth, 1976; Condie, 1986; Foley et al., 2002; Jahn et al., 1981; Martin, 1986; Moyen and Martin, 2012; Moyen and Stevens, 2006; Rapp et al., 1991, 2003; Springer and Seck, 1997; Zhang et al., 2013). The pressure–temperature conditions of melting are plotted on a simplified phase diagram for mid-ocean ridge basalt compositions (Fig. 3, right-hand column; modified from Hacker et al. (2003)); the “Amp in” and “Gt in” lines show the minimum stability fields of amphibole and garnet in mafic rocks, respectively (taken from Moyen and Stevens, 2006). In the experiment we identify three tectonic settings where melting of hydrated basalt and the generation of intermediate to felsic melts may occur: (1) where the lower crust delaminates and drips into the mantle (Fig. 3a); (2) where the crust locally thickens (Fig. 3b); and (3) where small-scale crustal overturns occur (Fig. 3c). We discuss each of these in more detail next.

3.2.1. Delamination and dripping of the lower crust into the mantle

The hot underplated basaltic melts derived from the mantle (pink in Fig. 3a) penetrate through the middle–lower crust in a dome-like fashion, triggering melt-assisted convection in the crust (Schenker et al., 2012). In the colder inter-domal crustal down-welling regions, local burial of the middle–lower crust toward the Moho occurs (red frame in Fig. 3a), which may also lead to delamination or dripping of this crust into the underlying mantle (blue frame in Fig. 3a). In both cases, the hydrated basalt undergoes partial melting due to conductive heating from the surrounding melt-bearing mantle or the underplated dry basaltic melts. In the case of the buried middle–lower crust, melting occurs at relatively low pressures between 0.5 and 1 GPa (red asterisks in Fig. 3a'). By contrast, although melting within the delaminated lower crust starts around 0.5 GPa, it is dominantly a higher pressure phenomenon that continues with increasing pressure during the process of delamination and dripping into the mantle (blue asterisks in Fig. 3a'). The temperature of melting varies from 700 to 900 °C. Thus, the parameters of melting mostly correspond to

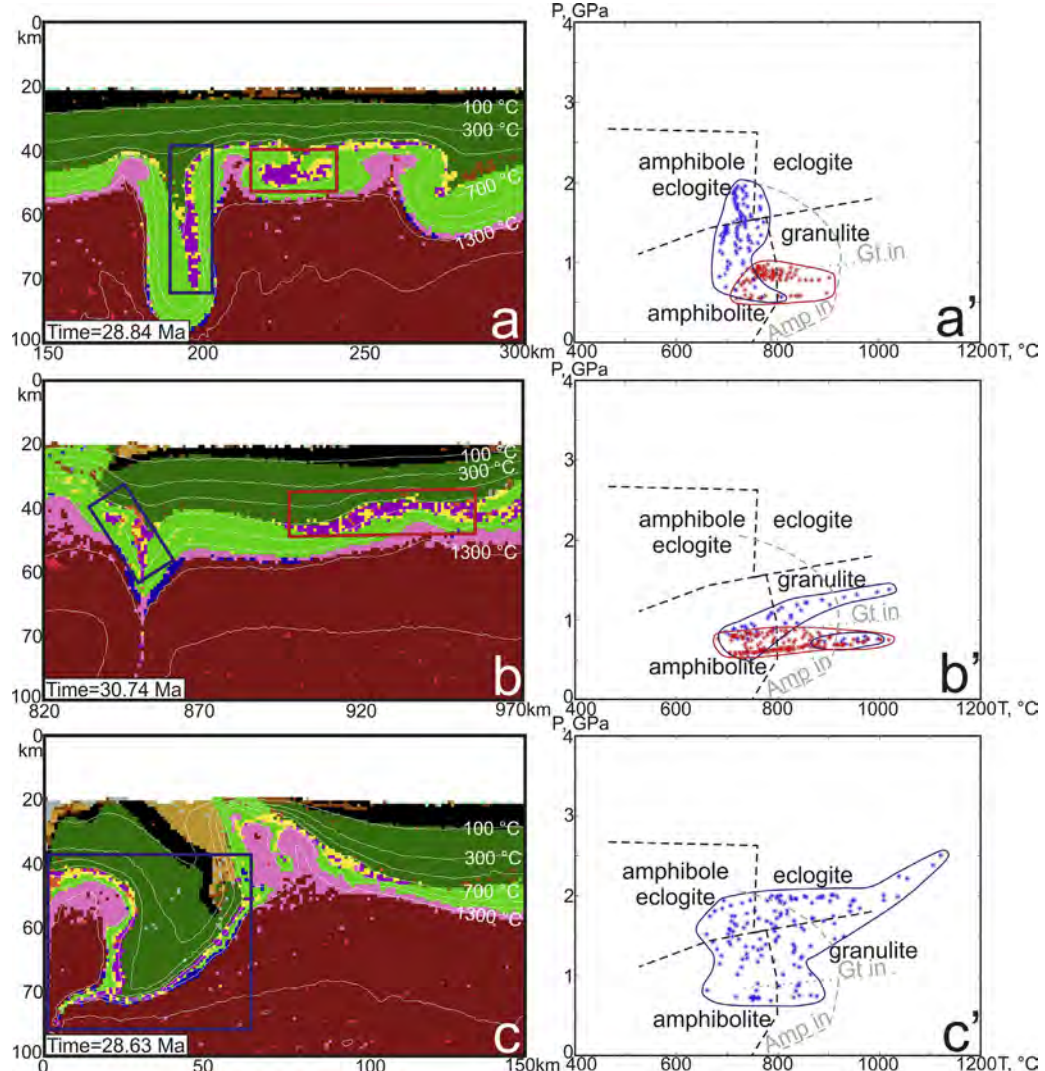


Fig. 3. Three representative snapshots (150 km × 100 km sections of the original 1000 km × 500 km model) to show the tectonic settings for partial melting of the hydrated basalt in the reference experiment: (a) delamination and dripping of the lower crust into the mantle; (b) local thickening of the crust; (c) small-scale crustal overturn. The pressure–temperature (P – T) conditions of melting for the crust outlined in the blue and red boxes in the snapshots on the left are plotted on a simplified phase diagram for mid-ocean ridge basalt in the right column (modified from Hacker et al., 2003); the “Amp in” and “Gt in” lines show the minimum stability fields of amphibole and garnet in mafic rocks, respectively (taken from Moyen and Stevens, 2006). (For interpretation of the references to color in this figure legend, the reader is referred to the web version of this article.)

the amphibolite facies with a smaller proportion occurring in the amphibole eclogite, eclogite and granulite facies (Fig. 3a'). In both cases, melting occurs within the amphibole stability field, but partial melting of the buried crust in inter-domal regions occurs at lower pressures, mostly outside the garnet stability field, whereas delamination-related melting occurs mostly at higher pressures within the garnet stability field.

3.2.2. Local thickening of the crust

The hot mantle that upwells and decompresses following the lower crust–upper mantle delamination produces new basaltic lavas at the surface (black in Fig. 3b), which together with local shortening (due to the rising underplated melts), leads to burial and local thickening of the pre-existing basalt in the upper–middle crust. Due to the elevated geotherms, the bottom part of this hydrated layer undergoes partial melting at middle-crustal depths (~20–30 km; red frame in Fig. 3b) or slightly deeper (blue frame in Fig. 3b). The melting occurs over a wide range of temperatures, from 700 to 1000 °C, but within a narrow interval of pressure, mostly between 0.5 and 1.5 GPa (Fig. 3b', both red and blue asterisks). Thus, melting occurs in the amphibolite and granulite facies, both outside and within the garnet stability field. In some cases, the local crustal thickening leads to lower crustal delamination.

3.2.3. Small-scale crustal overturns

The buoyant dry basaltic melt diapirs can also percolate though the entire crust up to very shallow upper-crustal levels. This penetration is enabled by the intense melt-induced crustal weakening prescribed in the model ($\lambda_{melt} = 0.001$). In turn, this may trigger an overturn of a small block of the crust located in between the melt diapirs. The overturn efficiently brings the upper-crustal hydrated basalt to the Moho and forces it to penetrate into the upper mantle (Fig. 3c). As a result, the relatively cold hydrated basalt block comes into direct contact with the hot melt-bearing mantle and undergoes partial melting at the base and from the sides (Fig. 3c). With time, due to gradual warming and eclogitization, the block sinks further into the mantle and undergoes almost complete melting. Melting along the margins of the overturned block occurs over a wide range of pressure and temperature (650–1100 °C and 0.7–2 GPa), mostly within the garnet stability field but both within and outside the amphibole stability field (Fig. 3c'). Melting within the sinking eclogitized crust gradually delaminating from the block occurs at relatively higher pressures and temperatures.

3.2.4. Discussion

In all these tectonic settings dacitic melts are extracted from the partially melted hydrated basalt derived from the upper–middle crustal layer. The small-scale crustal overturns and local crustal thickening produce most of dacitic melts. These melts form both dacite lavas (gray in Fig. 3) and plutonic bodies (orange in Fig. 3). Intruded melts crystallize and simultaneously or progressively form domes within the overlying mafic crust (e.g. Fig. 2e–g).

In addition, the model accounts for the extraction of residual dacitic melts from the gradually crystallizing underplated dry basaltic melts derived from the mantle. These residual melts are also split into volcanic (brown in Fig. 3) and plutonic (yellow in Fig. 3) units. The fractionated dacitic melts tend to stay at middle–lower crustal depths for a long time before they ascend, crystallize and form domes within the overlying mafic crust (brown in Fig. 2g), similar to the dacites derived by melting of the hydrated basalt.

Thus, the intermediate to felsic melts in the experiment are mostly produced by partial melting of the original hydrated basalts or by fractional crystallization of the underplated dry basaltic melts. By contrast, the contribution of the newly formed mantle-derived volcanic basaltic crust (black in Figs. 2 and 3) to the production

of the felsic crust is rather negligible in the experiment. Although this newly formed crust is involved in subduction, where it undergoes partial melting over a large range of pressures (to >3.0 GPa), the amount of melt produced is negligible due to the brevity of the subduction episode as well as the limited volume of subducted hydrated basalts. Part of the reason for the limited volume of hydrated basalts is erosion due to the slightly elevated topography of the oceanic-type crust just before subduction. Nonetheless, a small volume of subduction-related TTG melts might contribute to the diversity of Archean granitoids.

3.3. Long-term evolution of the continental crust

We also studied details of the long-term tectono-magmatic evolution of various sections of the intermediate to felsic crust formed during the experiment (Fig. 4). In particular, the dacitic melts derived from dry basalt that intrude into the middle–lower crust (yellow in Fig. 4a) mix with the melt-bearing hydrated basalt (violet in Fig. 4a) and the dacites derived from this basalt (orange in Fig. 4a). This layer may remain at this intermediate crustal level for tens of millions of years, undergoing re-melting and gradually creating partially molten domes. Due to the ongoing mantle convection, the intermediate to felsic layer may also be partly involved in delamination events, as shown in Figs. 2g and 4b. Furthermore, after partial solidification of the layer it can be re-melted due to the heat coming from the mantle upwellings (Fig. 4c), and thus may potentially produce melts that are even more SiO₂-rich.

During the experiment, the continuous production and remelting of the intermediate–felsic layer leads to the formation of felsic domes that penetrate the upper mafic crust (Figs. 4 and 5). The deeper and hotter partially molten lower part of the felsic layer facilitates the diapiric ascent by delivering new material into the regions of domal upwellings. The domes consist of dacite from hydrated basalt (gray when crystallized) and dacite from dry basaltic melts (brown when crystallized), or they represent a mix of melts from these two sources. The domes rise up into the shallow upper crust and may even become partly exposed at the surface by erosion. Blocks of crust that include a series of such domes within the hydrated basalt (blue and red frames in Fig. 5a) are separated by intrusions of dry basalt. At approximately 150 Ma the proportion of felsic domes in the continent-like crust varies both laterally and with depth, but mostly it is >50% (Fig. 5b,c). Because of the rarity of small-crustal overturns within this particular experiment, the dacite derived from dry basalt strongly prevails over the dacite derived from hydrated basalt. As the domes rise, the overlying basalt is moving downward, forming the archetypal dome-and-keel structure that dominates Archean granite–greenstone terranes (e.g. François et al., 2014; Van Kranendonk, 2011).

The series of large mantle upwellings that develops at the left-hand boundary of the model forces the continent-like crustal blocks to undergo shortening and amalgamation. The alternation of compression (due to oceanic-type plate advancing) and tension (above mantle upwelling zones) causes both deformation of the previously formed felsic domes and the formation of new domes, which slowly rise upwards on timescale of tens of millions years. The compression combined with the elevated geotherms contributes to the formation of a thick felsic melt-bearing layer, up to 20–30 km thick, when the continental-type plate is shortened to <200 km at ca. 170 Ma (Fig. 2h). The resulting felsic diapirs enable sagduction of the dry basaltic crust that previously separated continental-like crustal blocks containing felsic domes (e.g. Fig. 2h).

After the spontaneous subduction of the oceanic-type plate occurred, the shortened continental-type plate undergoes a period of slight extension caused by retreat of the subduction trench. The resulting continent-like crust represents a strongly deformed

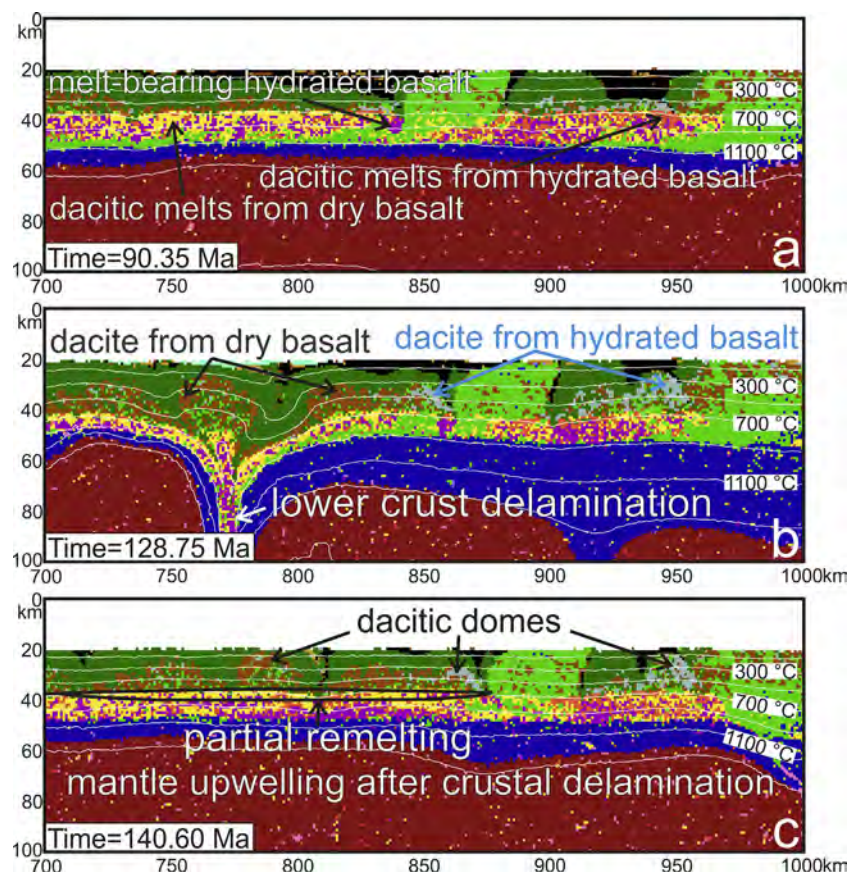


Fig. 4. Three representative time-slice snapshots (300 km × 100 km sections of the original 1000 km × 500 km model) to show the evolution of the melt-bearing layer located in the middle-to-lower crust in the reference experiment. The layer consists of the dacitic melts generated by the fractional crystallization of dry basaltic melts (yellow), the melt-bearing hydrated basalt (violet) and the dacitic melts (orange) extracted from the hydrated basalt (a). After formation, the layer gradually produces domes that penetrate the mafic crust and partly crystallize (b). Where this layer is involved in delamination events (b), the heat from the upwelling mantle causes remelting (c). (For interpretation of the references to color in this figure legend, the reader is referred to the web version of this article.)

mix of felsic (50–60%) and mafic (40–50%) domains without well-defined boundaries for the intrusive bodies (e.g. Fig. 2o). The subducted sediments and the subordinate hydrated basalts also undergo partial melting and are then exhumed toward the surface within the intra-arc and backarc regions.

Thus, during the evolution of the experiment we observe two distinct types of continent-like crust that develop sequentially: (1) a pristine granite-greenstone-like crust with dome-and-keel geometry formed over delaminating-upwelling mantle and mostly subjected to vertical tectonics processes (Figs. 4c and 5b,c); and

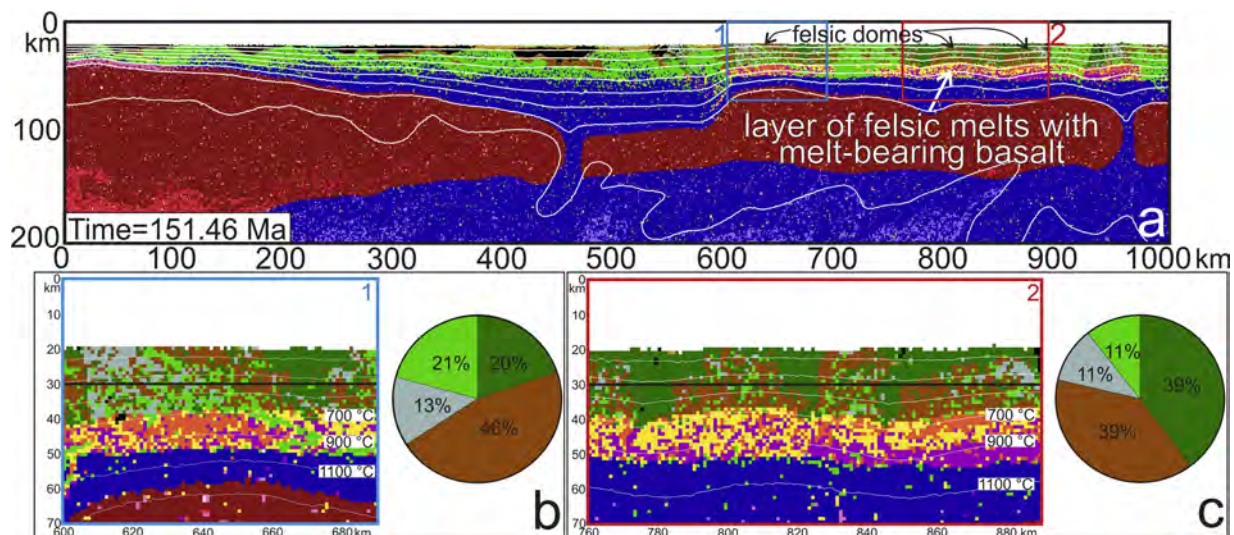


Fig. 5. Percentage of rock types that comprise the granite-greenstone-like crust with dome-and-keel geometry in the reference experiment. The percentage is shown for two blocks of the continental-like crust (b,c) that are separated by an intrusion of dry basalt (a).

(2) a reworked (accreted) crust containing strongly deformed granite-greenstone and subduction-related sequences and subjected to both strong horizontal compression and vertical tectonics processes (blue frame in Fig. 2h – the right-half of Fig. 2o). The reworked (accreted) continent-like crust was stretched and now comprises a large-scale tectonic mélange of several deformed and magmatically reworked blocks of pristine crust.

3.4. Evolution of the subcontinental lithospheric mantle

Although the existence of a compositionally buoyant and rheologically strong, highly depleted Archean subcontinental lithospheric mantle (SCLM) has long been recognized (e.g. Djomani et al., 2001; Jordan, 1978) together with possibility that it formed simultaneous with the overlying continental crust (e.g. Griffin et al., 2003), its origin remains contentious. Therefore, to better understand the origin of the SCLM we followed the evolution of the mantle in term of its movement, deformation, melting and depletion in the numerical experiment.

To account for the formation of the primordial mafic crust, we prescribed that all melt present in the mantle along the initial geotherm had been extracted. In addition, we prescribed this initial depletion to be no less than 10% down to 300 km depth (from mid blue to light orange in Fig. 6a). After the first few lithospheric

delamination–mantle upwelling events, the mantle depletion profile becomes more realistic with the most depleted mantle located directly below the Moho (from yellow to light orange in Fig. 6b). During the model evolution, as soon as the upper (most depleted) part of the mantle solidifies it may participate in the delamination (Fig. 6b,c). Due to the low density of this depleted mantle compared to the deep mantle, it rarely penetrates deeper than 200 km, and forms a return flow re-accreting to the bottom of the crust (Fig. 6c). Thus, due to the depletion-related mantle buoyancy, a tendency toward secondary convection exists in the depleted upper mantle layer, which interacts with deeper mantle upwellings. These deep mantle upwellings (plumes) forming at the lower boundary repeatedly bring more fertile mantle to shallow sub-crustal levels (Fig. 6c). The deeply buried depleted mantle forming part of lithospheric drips can also be heated at the lower boundary and partly returned to shallow depths, thus re-accreting to the depleted SCLM layer (Fig. 6c).

The sequence of large mantle upwellings that occur at the left-hand boundary of the model (Fig. 6d) generate a push that advances the oceanic-type lithospheric plate, which creates more vigorous lateral mantle mixing beneath the continental-type plate (d,e). Thus, the combination of extensive delamination with mantle upwelling events, together with the lateral shortening, allows SCLM that forms over a period of 100 Ma to become well mixed

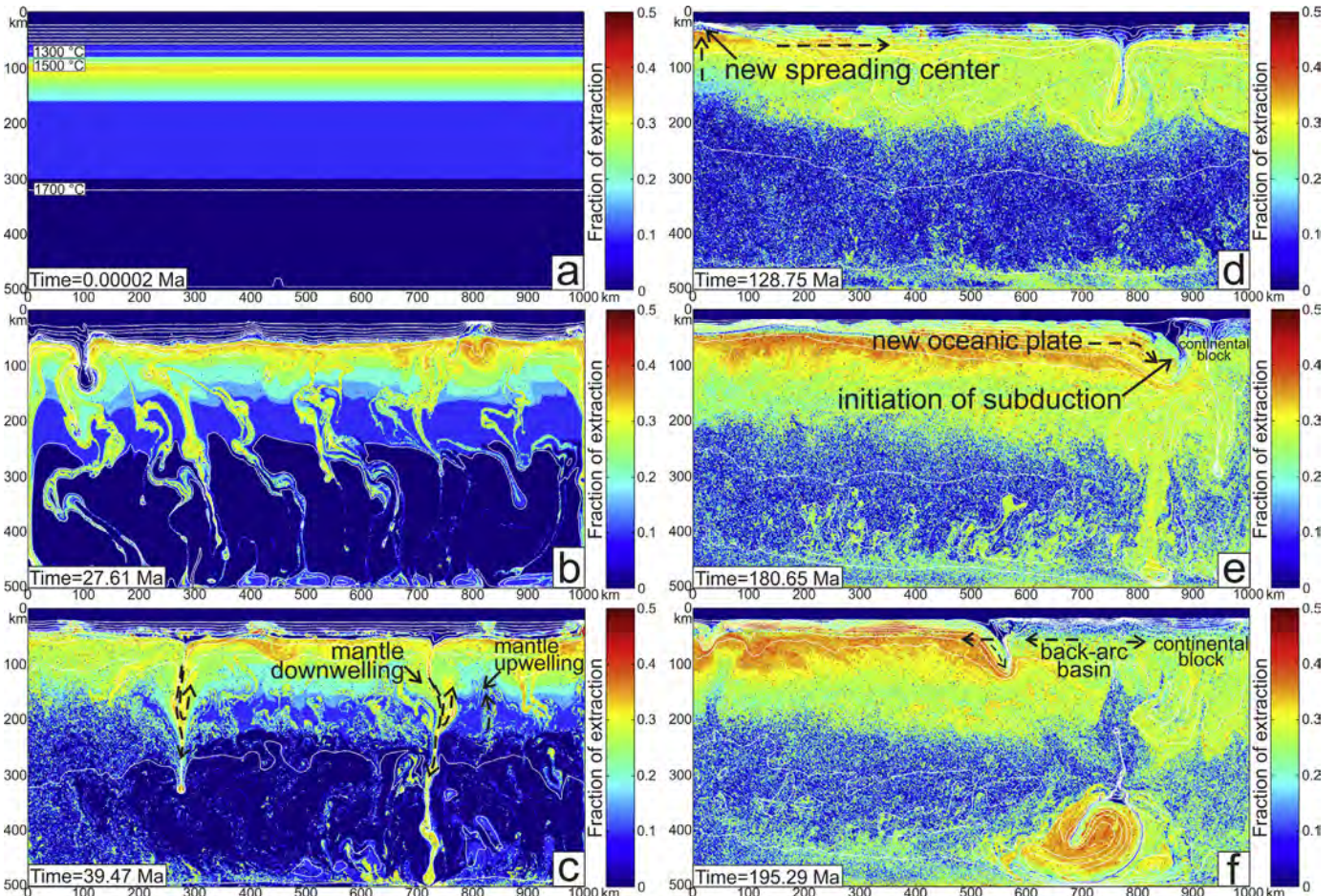


Fig. 6. Representative time-slice snapshots to show the evolution of melt extraction from the mantle (i.e. the degree of melt depletion) during the reference experiment. Initially the most depleted upper mantle is located at 80 km depth (a). After the first 25 Myrs of evolution, the most depleted zone moves up to lie immediately below the Moho (b). As soon as the upper (most depleted) part of the mantle solidifies it may participate in delamination events (b,c), but due to its low density it rarely penetrates deeper than 200 km, and forms a return flow re-accreting to the bottom of the crust (c). The combination of extensive delamination with mantle upwelling events together with the lateral shortening due to the advance of the oceanic-type plate allows the mantle beneath the continental-like crust that formed over a period of 100 Ma to be well mixed with an average degree of depletion of 0.25–0.3 at a final thickness of 200 km (d,e). The mantle forming part of the advancing oceanic-type plate is more highly depleted at 0.35–0.40 fraction of melt extracted (d,e). Subsequent heterogeneities within the lithospheric mantle are related to the subduction of the oceanic-type lithospheric plate beneath the continental-like lithospheric plate (f).

with an average degree of depletion of 0.25–0.3 at a final thickness of 200 km (e.g. the uppermost mantle in the right-hand half of Fig. 6d,e). On the other hand, after the transition to the subduction regime, we assume that the SCLM may undergo modifications due to slab-related mantle rehydration and upwelling fertile mantle (Fig. 6f). However, since the lower boundary in our experiment is relatively shallow (500 km), the involvement of the subducted oceanic-type lithospheric material into the mantle convection could be overestimated.

Due to decompression melting, the hot mantle upwellings generate a highly depleted peridotite characterized by up to 0.35–0.45 melt extraction with a thick mafic crust on top (e.g. the uppermost mantle in the left-hand half of Fig. 6d). This mantle does not delaminate but instead gradually cools, forming a colder ocean-type lithosphere on the left compared to the hotter continental-like lithosphere on the right-hand side (Fig. 6d,e). Note, that due to the shallow melting conditions, oceanic-type mantle lithosphere is more depleted than the SCLM forming underneath the continental-like domain. As soon as the subduction of this cold depleted oceanic-type lithospheric plate is initiated, it is maintained by the density increase owing to the transformation of the thick mafic crust to eclogite. Due to the positive chemical buoyancy of the strongly depleted oceanic mantle and very inhomogeneous crustal thickness, composition and strength of the oceanic-type plate, the subduction episodes are short-lived and frequently terminate by slab breakoff (Fig. 6f).

3.5. Influence of model parameters

Parameter space for our complex tectono-magmatic reference model is relatively large. Therefore, in this section we describe additional representative numerical experiments in which the physical parameters have been changed within plausible values. These changes produce significant differences in model results, which are summarized in Table 2.

3.5.1. Higher mantle temperature

Three experiments from Table 2 were run with a higher mantle temperature (300 °C above the present-day value, compared with 250 °C in the reference model) and in one case a higher radiogenic heat production (increased by a factor of 3 rather than 2) for the upper-mantle. In these experiments, felsic melts are generated from the original hydrated basaltic crust in tectono-magmatic settings similar to those in the reference model, including delamination of the lower crust, small-scale crustal overturns, and local thickening of the crust (cf. Figs. 3, 7b,d and 8a; experiments try85, try83, try55 in Table 2). The main distinctions between these experiments and the reference model are an increase in the volume of underplated dry basaltic melts (Fig. 8a) and the appearance of large-scale crustal overturns (Figs. 7b,d and 8a) instead of subduction as a result of the hotter mantle, and consequently an increase in the frequency of mantle upwellings.

3.5.2. Crustal composition and strength

In experiments where the initial crust is composed of a thicker (30 km) dry basalt layer and thinner (10 km) hydrated basalt layer (experiments try105 and try109 in Table 2), the crust is stronger compared with that in the reference model, which produces a very stable geodynamic regime without pronounced diapiric upwellings initiated by undepleted melts (cf. Figs. 2d and 8a–c). The increase in crustal strength makes it hard for the underplated dry basaltic melts to rise through the overlying mafic crust in a diapiric manner. In turn, this leads to less efficient delamination of the lower crust and the absence of small-scale crustal overturns during the evolution of the experiments (Fig. 8b,c). Only rare large mantle diapirs, which generate a thick hydrated basaltic crustal layer at the

top, and underplated melts trigger more vigorous crustal diapirism, reworking and delamination. After these rare events the evolution of the experiments is similar to the evolution of the reference model (experiment try105 in Table 2).

If, in addition to the thick dry basalt layer, the ratio of volcanic to plutonic rocks is increased to 40:60 (experiment try109 in Table 2), the volume of underplating dry basaltic melts decreases notably, which reduces further the frequency of delamination events, and crustal overturns are absent (Fig. 8c). By contrast, an increase in the thickness of the hydrated basalt layer in the initial crust and a reduction in the thickness of the dry basalt layer (experiment try110 in Table 2) causes intense early crustal replacement by dry basaltic melts within first ca. 40 Ma of the evolution. However, this vigorous activity is transient and later in the evolution the resulting crust is composed of mostly dry basalt with a subordinate amount of hydrated basalt and dacite (Fig. 8d). This crust experiences progressive cooling during the following 200 Ma.

3.5.3. Conditions of melting

In another series of experiments (listed after try110 in Table 2), we used hydrated basalt for the composition of the original crust and the wet basalt solidus for crystallization of the mantle-derived melts. The upper-mantle temperature for these experiments is the same as the reference model (250 °C hotter than the present-day value), but the lower boundary temperature is variable. An initial high Moho temperature (1570–1590 °C) combined with a very hot adiabatic temperature profile in the middle–lower crust (see Fig. 9a,c) triggers intense crustal convection and cooling within first 10–15 Ma. After this period of intense activity, the lithospheric temperature profile stabilizes with a Moho temperature of ~1200 °C. The whole 40 km thick crust is represented by hydrated basalt, more than half of which is partially melted due to the hot initial thermal structure of the crust (Fig. 9a). The melt-bearing layer of hydrated basalt together with the mantle-derived hydrated basaltic melts creates more favorable conditions for crustal overturns (e.g. Fig. 9b) than underplating dry basaltic melts in the first series of experiments. We also investigated the effect of increasing the solidus temperature of the basaltic residue after the hydrous dacitic melt extraction (from the wet to the dry basalt solidus; Fig. 9c). In this case, after the first 10–20 Ma, the evolution the lower crust is controlled by the residues from melting, which makes a strong lower crust and reduces the number of crustal overturns (Fig. 9d). Only rare large mantle diapirs generate additional hydrated basalt melts that rise into the crust and dry basaltic melts that underplate the crust, causing intensive small-scale crustal overturns and delamination, and producing dacitic melts. Consequently, later in the evolution the experiments with strong lower crustal residues behave similarly to the experiments with thick dry basaltic crust (cf. Figs. 8b–d and 9d).

In this series of experiments, the one with a volcanic to plutonic rock ratio of 100 (ttag in Table 2; Fig. 9e,f) is characterized by the accumulation of basalt on the surface, which crystallizes rapidly leading to a very cold thermal structure of the crust. This is inconsistent with the high apparent thermal gradients registered in the early Archean crust (Brown, 2014). The last two snapshots in Fig. 9g,h are taken from an experiment where the rheology of the mantle was changed based on the presence of melt. In this experiment, suprasolidus mantle was assigned a relatively strong dry olivine rheology if there was no melt present (i.e. $M < 0$ in Eq. (5)). Surprisingly, such rheological strengthening of depleted mantle did not lead to any significant differences in the evolution of this experiment compared with the reference model evolution, and both delamination of lower crust and small-scale crustal overturns are typical (cf. Figs. 2d and Fig. 9h).

Table 2
Influence of model parameters.

Model	Model width (km)	Model height (km)	$\Delta T_{\text{mantle}}^{\text{a}}$	T_{Moho} (°C)	H_r	Thickness of hydrated basalt layer (km)	Thickness of dry basalt layer (km)	Dacite initial	Volcanic/plutonic ratio	Lower boundary temerature (°C)	Comments	Results
try85	1000	500	250	1200	x3; mantle x2 ^b	20	20	–	20/80	2040	The reference experiment	Delamination, small-scale crustal overturn, mantle diapirs, subduction. Transition from Crust I to Crust II ^c (Fig. 2)
try83	1000	500	300	1200	x3; mantle x2	20	20	–	20/80	2040		Delamination, more frequent small-scale crustal overturns, mantle diapirs, large-scale resurfacing. Crust I is not preserved. Fragments of Crust II (Fig. 9)
try55	1000	500	300	1200	x3	20	20	–	20/80	2040		Delamination, more frequent small-scale crustal overturns, large mantle diapirs. Crust I is partly transformed to Crust II (Fig. 8a)
try91	1000	500	300	1200	x3; mantle x2	10	30	–	20/80	2040		Delamination, small-scale crustal overturns, no big diapirs. Crust I is partly transformed to Crust II
try105	1000	500	250	1200	x3; mantle x2	10	30	–	20/80	2040		Stagnant-lid regime during first 100 Ma. Than few mantle diapirs, delamination, few small-scale crustal overturns, short-lived subduction event. Crust I is partly transformed to Crust II (Fig. 8b)
try109	1000	500	250	1200	x3; mantle x2	10	30	–	40/60	2040		Few delamination events, no crustal overturns, stagnant-lid regime during 270 Ma (Fig. 8c)
try110	1000	500	250	1200	x3; mantle x2	30	10	–	20/80	2040		Large mantle upwelling zones cause intensive crustal reworking including small-scale overturns, and delaminations, and lead to vigorous underplated dry basaltic melts diapirism. The resulted crust inreached in dry basalt stabilizes and keeps stagnant-lid regime (Fig. 8d)

Table 2 (Continued)

Model	Model width (km)	Model height (km)	$\Delta T_{\text{mantle}}^{\text{a}}$	T_{Moho} (°C)	H_r	Thickness of hydrated basalt layer (km)	Thickness of dry basalt layer (km)	Dacite initial	Volcanic/plutonic ratio	Lower boundary temperature (°C)	Comments	Results
ttacd	1000	300	250	1580	x2	40	–	–	20/80	1900 + large temperature fluctuation	Mantle derived melts are hydrated basalt. Mantle depletion is not taken into account.	Intensive small-scale crustal overturns, delamination. Crust I (Fig. 9a,b)
ttaci	1000	300	250	–//–	x2	40	–	–	20/80	–//–	+Dry basalt residue ^d	Stronger crust. Less small-scale crustal overturns delamination. Crust I (Fig. 9c,d)
ttaf	500	300	250	–//–	Present-day values	30	–	10	20/80	–//–	–//– +Mantle depletion ^e	Few small-scale crustal overturns. Felsic domes within a mix overlying crust.
ttag	500	300	250	–//–	–//–	30	–	10	100/0	–//–	–//–	A marble cake crust composed by dacite and basalt, few small-scale crustal overturns with partial crustal remelting (Fig. 9e,f)
ttajy	500	500	250	1580	x2	30	–	10	10/90	2140 –//–	–//–	Delamination, small-scale crustal overturns, more mantle diapirs, large mantle diapir causes large crustal overturns. Felsic domes within a mix overlying crust.
ttajzc	500	500	250	–//–	x2	30	–	10	20/80	2040 –//–	–//–	Few mantle diapirs, single overturn. Few felsic domes within a mix overlying crust
ttbjca	500	500	250	1590	x2	30	–	10	10/90	2140 –//–	–//–	Delamination, small-scale crustal overturns. Felsic domes within a mix overlying crust
ttbjhe	500	500	250	1570	x2	30	–	10	10/90	2040 –//–	–//– Less melt-bearing rocks ^f	Delamination, small-scale crustal overturns. Felsic domes within a mix overlying crust (Fig. 9g,h)

^a ΔT_{mantle} – a difference between the prescribed upper-mantle temperature in the experiments and the average present-day value.^b Radiogenic heat production for all rocks is increased by a factor of 3 (except for the peridotite, which is increased by a factor of 2 to avoid mantle overheating).^c Crust I – granite-greenstone-like crust with dome-and-keel geometry mostly subjected to vertical tectonics processes; Crust II – a reworked (accreted) crust subjected to both strong horizontal compression and vertical tectonics processes.^d Dry basalt residue – the type of the residue is changed to dry basalt after 30% of melt extraction from the melt-bearing hydrated basalt.^e The density of the mantle is decreasing due to the melt extraction (similar to the reference model).^f Solid lithologies were changed to the melt-bearing analogs when $M_0 > 0$ and $M > -0.01$ (for other experiments when $M_0 > 0$), where M – the amount of melt available at each marker, M_0 – the equilibrium volumetric degree of melting computed at this step as the function of P, T and rock composition, $M = M_0 - \sum_n M_{\text{ext}}$, where $\sum_n M_{\text{ext}}$ is the total melt fraction extracted during the previous n extraction episodes.

–//– – the parameter is the same as in the previous experiment.

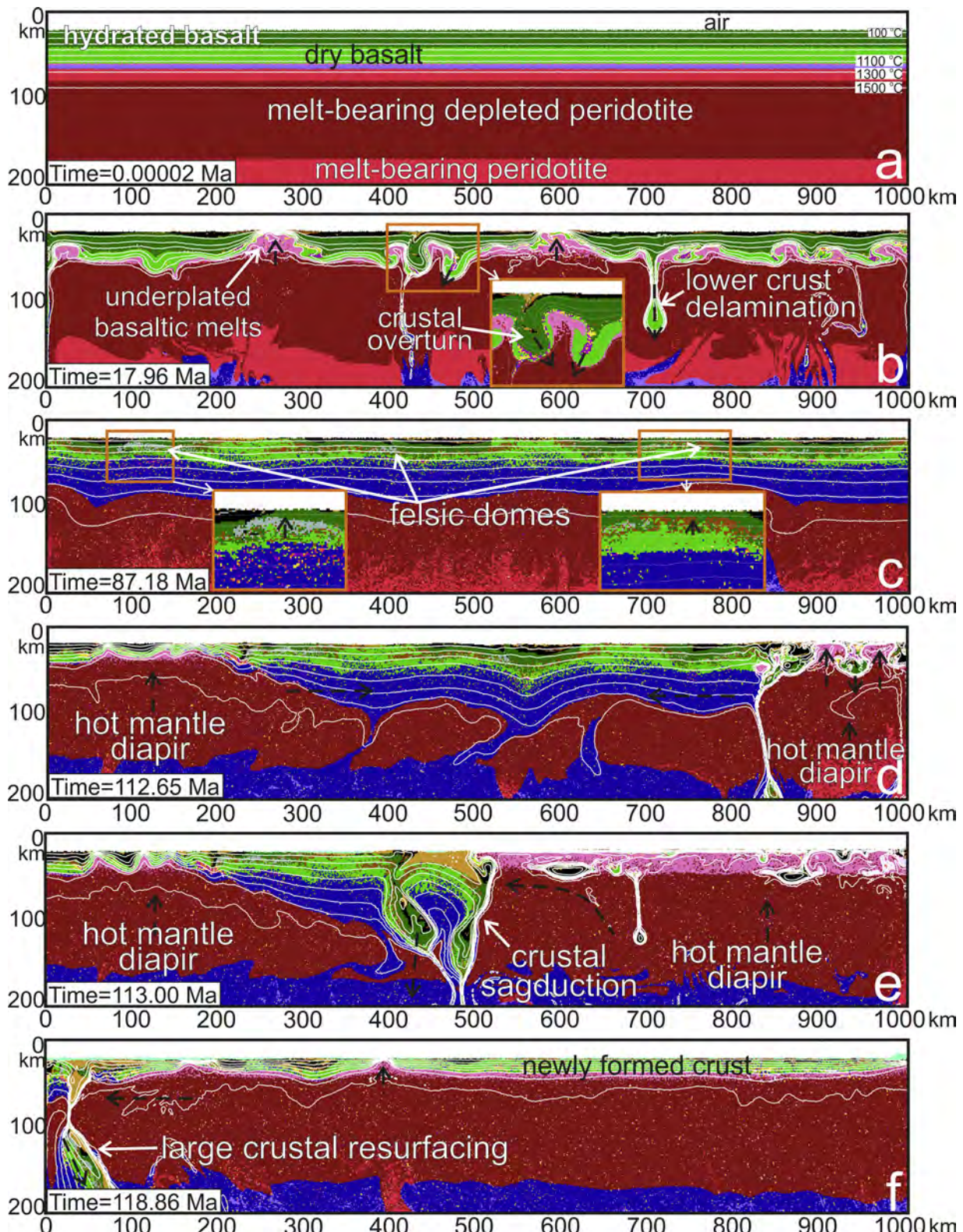


Fig. 7. Representative time-slice snapshots to show evolution of an experiment with an upper-mantle temperature 300 K higher than the present-day value (experiment try83 in Table 2). By c. 18 Myrs the simultaneous upwelling of the melt-bearing depleted mantle (initially located at depth (a)) and delamination of the mantle lithosphere and part of the lower portion of the mafic crust has begun (b,c). Mantle upwellings lead to dry basaltic magmas underplating the lower crust (pink) and the formation of new hydrated basaltic lavas atop the crust (black) (b). Rising dry basaltic melts may lead to crustal overturn or lower crustal delamination (b), and cause partial melting of the hydrated basalt (violet). Felsic melts extracted from the melt-bearing hydrated basalt and those generated by the fractional crystallization of dry basaltic melts mix with the melt-bearing basalt and localize at the bottom of the basaltic crust, where they create domes within the overlying mafic crust in the same way as happens in the first experiment (c). From c. 110 Ma, a large mantle upwelling occurs at each side of the model (d) and destroy the existing continental-like plate, which sinks into the mantle (e,f), within 6 Ma. (For interpretation of the references to color in this figure legend, the reader is referred to the web version of this article.)

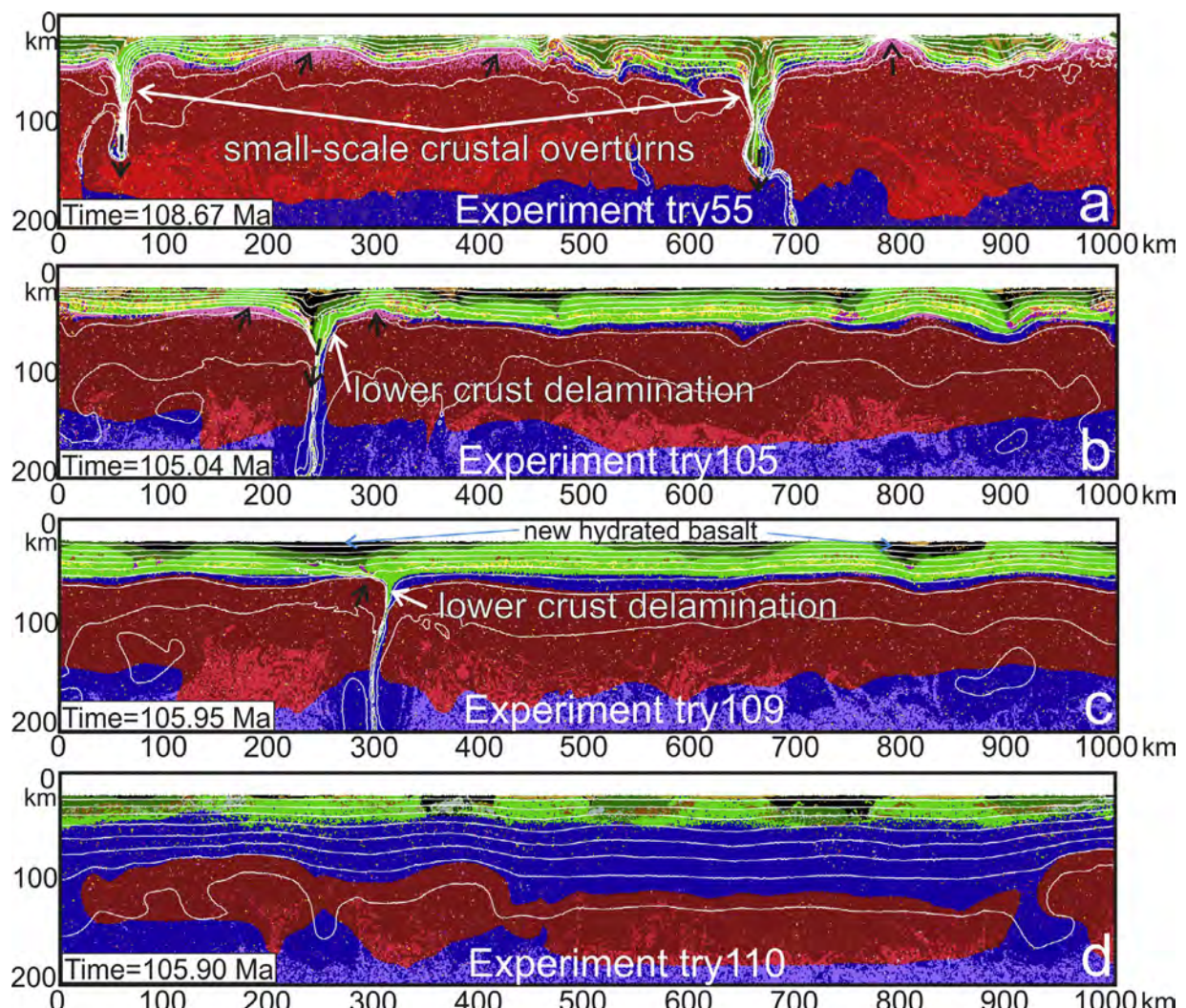


Fig. 8. Representative snapshots from some additional experiments (see Table 2 for details of the initial set-up and Section 3.5 for discussion): (a) experiment try55; (b) experiment try105; (c) experiment try109; (d) experiment try110. Colors are the same as Fig. 1. (For interpretation of the references to color in this figure legend, the reader is referred to the web version of this article.)

3.5.4. Summary

The additional experiments were run to assess differences in geodynamic behavior due to changes in the model parameters compared with the reference model. In a majority of these experiments multiple small-scale crustal overturns, crustal thickening, and delamination were common. Similar to the reference model, they occur over delaminating-upwelling mantle. The intensity of the small-scale crustal overturns is strongly controlled by the amount and distribution of the underplated mantle-derived melts as well as by the compositional/rheological structure of the crust. These crustal overturns, which are triggered by mantle upwellings, are a periodic feature during the long-term stability of this tectono-magmatic regime, which we refer to as a stagnant-deformable lid regime.

This hotter regime is not typically characterized by intensive mantle cooling that leads to the periodic appearance of large hot mantle diapirs that break the overlying plate. Rather, there are two different types of behavior. Either an oceanic-type plate is developed that may subsequently subduct, as seen in the reference experiment, or a large-scale crustal resurfacing event may occur due to intensive decompression melting, as is typical in the higher temperature experiments (e.g. experiments try83, try55 in Table 2). It is the parameters of the experiment, such as the mantle

temperature, crustal rheology, and lower-boundary temperature, that determine the behavior, and in the reference experiment lead to episodes of short-lived subduction rather than large-scale crustal overturns. The location and the scale of subduction depend on the input parameters. As a result of episodic subduction, the granite-greenstone-like crust (Crust I in Table 2), which develops over the linked delaminating-upwelling zones in the mantle, is episodically reworking (the reworked crust; Crust II in Table 2) due to the predominantly horizontal tectonic processes associated with subduction, although undeformed blocks of Crust I may be preserved.

4. Discussion

The geodynamics of Earth in the Archean is a matter of current debate (O'Neill and Debaille, 2014) and the genesis of the early continental crust remains contentious (Herzberg and Rudnick, 2012; Johnson et al., 2014). Geodynamic modeling of the Archean using higher mantle temperatures and higher internal heat production has shown that subduction was unlikely before the Mesoarchean, which has led to the suggestion that the predominant geodynamic regime prior to the Mesoarchean was stagnant-lid plate tectonics, perhaps with resurfacing and/or intermittent subduction events

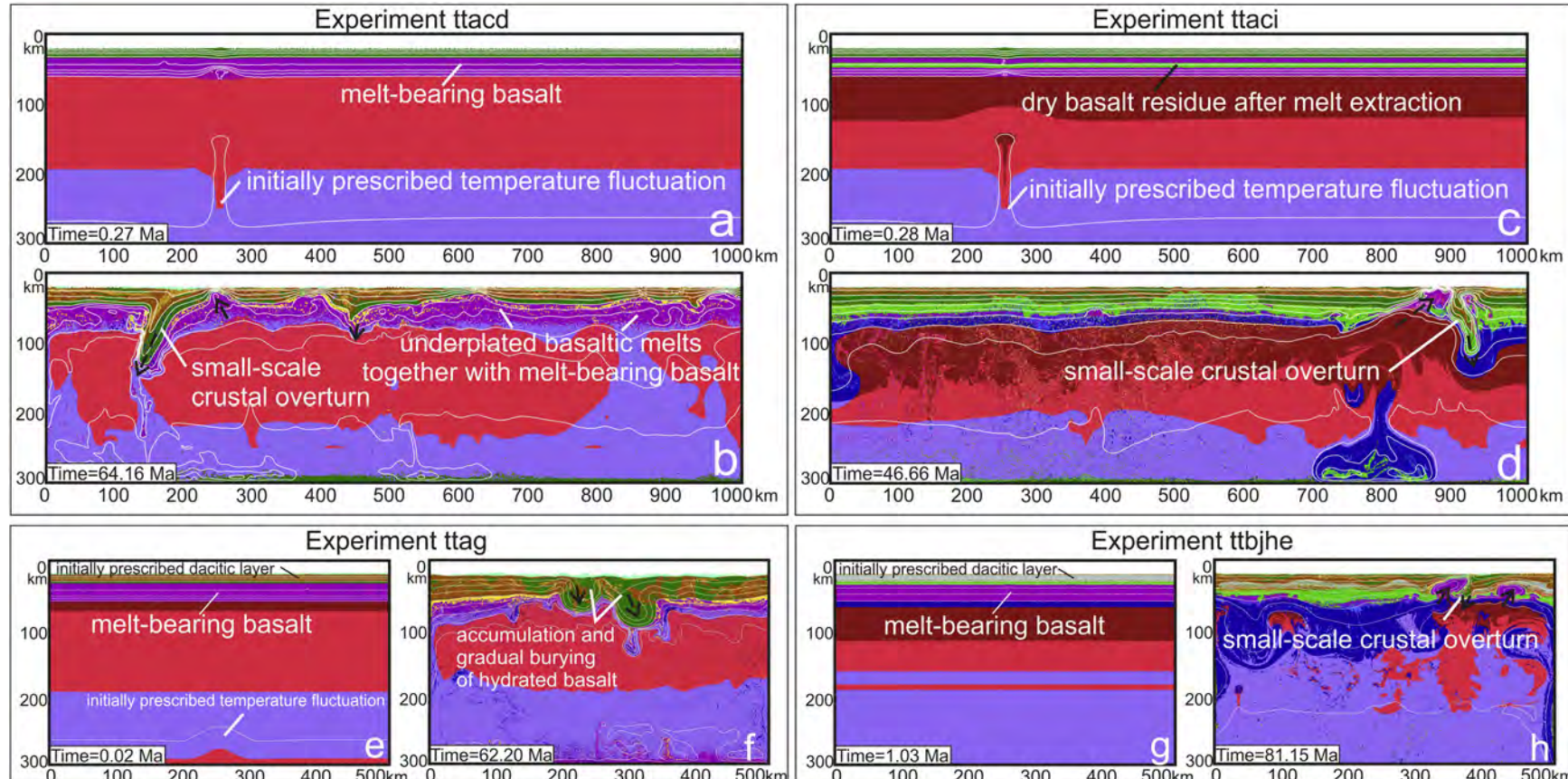


Fig. 9. Snapshots of the initial set-up and representative time-slice snapshots for some additional experiments (see Table 2 for details of the initial set-up and Section 3.5 for discussion): (a,b) experiment ttacd; (c,d) experiment ttaci; (e,f) experiment ttag; (g,h) experiment ttbjhe. Colors are the same as Fig. 1. (For interpretation of the references to color in this figure legend, the reader is referred to the web version of this article.)

(e.g. O'Neill et al., 2007a,b; Sizova et al., 2010; Van Hunen and van den Berg, 2008; Van Thienen and Van den Berg, 2004). The Archean crust is largely made up of gray gneisses, which are dominated by the tonalite–trondhjemite–granodiorite (TTG) suite with subordinate granite. The TTGs have a distinctive geochemistry that reflects derivation from plagioclase–garnet amphibolite, garnet-rich, plagioclase-poor amphibolite, and rutile-bearing eclogite with increasing pressure (Moyen, 2011). This variety has been argued to reflect a range of geothermal gradients perhaps generated in different tectonic settings (Moyen, 2011).

Given the variation in geochemistry noted above and the different tectonic settings postulated for the generation of silicic rocks (Moyen and Martin, 2012), our experiments were set up for conditions appropriate to the Eoarchean–Mesoarchean and designed to discover all possible tectonic scenarios in which felsic rocks could be generated under these conditions. Based on the experiments using a 2D petrological–thermomechanical numerical model, we have identified a variety of contemporaneous tectonic mechanisms that could lead to melting of primary and/or secondary crust and the production of silicic magmas. These mechanisms could have generated the range of TTG compositions preserved in the Archean continental crust.

4.1. Composition of felsic melts

For simplicity, we have called all intermediate to felsic melts derived from the mafic substrates in the model dacites. We do not deal directly with the chemistry of the melts within the modeling. However, since we know the P – T (pressure–temperature) conditions of melting in the different tectonic settings that develop during the experiments, we may use results from experimental petrology to assess the types of granitoids produced from the various source lithologies in each tectonic setting in the model. Thus, we are able to relate the general chemical composition of the dacitic melts generated in the experiments to models for the generation of TTG magmas in the literature.

As discussed above, the commonly accepted model for the generation of TTGs is by melting of hydrous metabasalt at garnet amphibolite, granulite or eclogite facies conditions. In the experiments, many of the dacitic melts forming plutons were produced from hydrated basalt at P – T conditions >1.0 GPa and 700–1000 °C (Fig. 3); they are likely to have had compositions similar to many TTG suites. These dacites were produced during lower crustal delamination and dripping of the lower crust into the mantle, and also during small-scale crustal overturns (blue frames in Fig. 3), whereas local thickening or heating of the crust most likely produced dacites equivalent to lower pressure TTG suites (red frames in Fig. 3).

However, many of the dacitic plutons in the reference model were produced from melting of gabbro (dry basalt) or fractionated from underplated dry basaltic melts. In these cases, the temperature of formation of the melts is rather high (1100–1200 °C) and the environment of melting or fractionation is not hydrous, as required for the formation of TTG melts. There does not seem to be any record of such high-temperature melts in the Archean geological record. Unless melting occurred under oxidizing conditions, the fractionated melts may not even be dacite in composition, but may have a more intermediate initial composition (Carmichael, 1964).

One potential mechanism to provide hydrous and oxidizing conditions for melting is via a large-scale resurfacing event. Such large-scale resurfacing events occurred in the models of mantle convection reported by Van Thienen and Van den Berg (2004). These resurfacing events involve a large section of the lithosphere (>1000 km long) that sinks into the mantle in less than 2 Ma, triggered by conversion of a sufficient volume of lower crust to eclogite to initiate the instability. Similar events were observed in our

experiments run at higher upper-mantle temperature than the reference experiment (300 °C vs 250 °C above the present-day value). In some of these experiments, after 100–150 Ma of predominantly stagnant-deformable lid behavior with short bursts of surface tectono-magmatic activity that generated granite–greenstone-like crust (e.g. Fig. 7a–c; Table 2), large and hot mantle plumes arise and over a period of 5–10 Ma destroy the existing continental-type plate as it sinks into the mantle (Fig. 7d–f; Movie 2). If such a process did occur on Earth prior to the period of major growth of the continental crust, it should have had an impact on the subjacent shallow mantle and could have resulted in oxidizing conditions during melting.

One way or another, the intermediate composition melts derived by fractionation from underplated dry basaltic melts remain in the middle and lower crust, where they may hybridize with other melts during the process of melting-assisted crustal convection (Figs. 3, 4). In turn, these various hybrid melts form domes in the upper crust (left-hand side of Fig. 4b,c), similar to those formed by the dacites derived by melting of the hydrated basalt (right-hand side of Fig. 4b,c). Once crystallized, the lower part of these domes may be remelted due to conductive heating from the hot mantle upwellings and/or from the associated underplated dry basaltic melts (Fig. 4c). These progressive remelting events will promote a change to more felsic melt compositions, ultimately producing potassic granitoids, which comprise 10–15% of Archean granitoids (Moyen, 2011; see also Moyen and Martin, 2012). Within the accreted continental crust (blue frame in Fig. 2h), where most of the dacite domes are strongly deformed, especially vigorous remelting occurs during heating associated with the crustal thickening. This is consistent with modern processes and experimental studies, which indicate that potassic granitoids in gray gneiss terranes are generally formed by remelting of older TTG crust (e.g. Moyen et al., 2007; Moyen and Martin, 2012).

In the dataset of gray gneisses compiled by Moyen (2011; see also Moyen and Martin, 2012) there are also examples of TTGs with enrichments in Mg, Ni and Cr relative to experimental melts of basalt. Such TTGs have been used in arguments for a subduction related mechanism for the generation of TTG magmas in the Archean, with the enrichments being explained by interaction between a basalt-derived TTG melt and the overlying mantle wedge through which it must pass if subduction was analogous to the contemporary Earth (e.g. Martin and Moyen, 2002; Rapp et al., 2010). Furthermore, Moyen and Martin (2012) emphasize that other, non-subduction models fit the petrological constraints, as argued long ago by Smithies (2000), particularly higher degrees of melting of the same source or hybridization with mafic melts (Moyen and Martin, 2012).

In our experiments, partial hybridization between different dacitic melts occurred in the middle and lower crust, where melts derived by fractionation from the underplated dry basaltic melts mix with melts derived from partial melting of the hydrated basalt. There are also tectonic settings where dacitic melts could have interacted with the adjacent mantle peridotite to generate enrichments in Mg, Ni and Cr. In particular, such interactions could occur during small-scale crustal overturns. The dacitic melts produced from partial melting of the hydrated basalt in the overturned block of the original upper-middle crust shown in Fig. 3c are likely to come into contact with the surrounding hot melt-bearing depleted mantle. Thus, these melts could interact with the mantle in a similar fashion to melts rising through a mantle wedge. Finally, spontaneous subduction of the oceanic-type lithospheric plate allows for melting and interaction of these melts with the adjacent mantle (Fig. 2i–o). The appearance of sanukitoids in the late Archean geological record may reflect this style of subduction, which would become more common during the transition to a global subduction regime as suggested by Laurent et al. (2014).

4.2. Crustal structure

Over the run time of the reference experiment the crustal structure is mostly characterized by the sequential development of two different types of crust. An early-formed granite–greenstone-like crust with dome-and-keel geometry is formed as a result of the reworking the thick basaltic crust into a more felsic crust by the processes of delamination, melting, magmatism and deformation. The granite–greenstone-like crust develops by vertical tectonic processes that occur over linked delaminating–upwelling zones in the mantle. The heat advected to the base of the crust by the upwelling mantle combined with the intrusion of hot mantle-derived melts into the crust leads to melting of the primary basaltic crust and the generation and extraction of dacitic melts. These melts are emplaced at depth in the crust and together with dacitic melts derived by fractionation from dry basaltic melts slowly start to rise diapirically, crystallizing from the top while remaining partially molten at the bottom, in an alternating regime of compression and tension (e.g. Figs. 4b and 5). The rising diapirs of dacite cause simultaneous sinking of the overlying mafic crust in a sagduction-like fashion modeled by Thébaut and Rey (2013). To a varying degree, these processes form a granite–greenstone-like crust above in most of the experiments we report here (Table 2 and Figs. 8 and 9). By contrast, a later reworked crust is formed as the result of predominantly horizontal tectonic processes that are terminated by a short-lived subduction event. This intensive crustal shortening and thickening event results in preservation of the felsic material as the mafic material is lost by dripping into the mantle (blue frame in Fig. 2h). The reworked crust is developed in experiments associated with both short-lived subduction and large-scale crustal overturns (Table 2).

The duality of crustal types produced in the experiments has parallels with different types of crustal domains recognized in Archean cratons. In an early interpretation, Windley and Bridgwater (1971) proposed that greenstone belts and associated granites characterized by lower-grade metamorphism represented high-level (upper crustal) terranes, whereas catazonal gneisses characterized by higher-grade metamorphism represented deep-level (lower crustal) terranes. By contrast, Van Kranendonk (2010) argued for two different types of crust, one type formed over upwelling mantle and another type associated with subduction, and proposed that Paleoarchean Earth was similar to modern Earth, with differences being the result of differences in mantle potential temperature, size of crustal plates, thickness of oceanic lithosphere and differences in crustal rheology.

Granite–greenstone domains, such as the East Pilbara Terrane of the Pilbara craton in Australia, the Barberton granite–greenstone belt in South Africa and the Superior Province in Canada, contrast with the gneissic terranes that comprise the West Greenland part of the North Atlantic craton. The inferred geodynamic settings proposed for these crustal domains vary from sagduction and crustal diapirism associated with upwelling mantle (e.g. the East Pilbara terrane (Thébaut and Rey, 2013; Van Kranendonk, 2010; Van Kranendonk et al., 2007); the Barberton granite–greenstone belt (Van Kranendonk, 2011; Van Kranendonk et al., 2009, 2014)) to plate margin processes (e.g. the Barberton granite–greenstone belt (Cutts et al., 2014; Moyen et al., 2006); the Superior Province in Canada (Percival et al., 2012); West Greenland (Nutman et al., 2007, 2013; Van Kranendonk, 2010)) and non-uniformitarian models (e.g. the Superior Province in Canada (Bédard and Harris, 2014)).

Of the granite–greenstone domains listed above, the East Pilbara terrane, which is characterized by dome-and-keel structures, is probably the least contentious. Crust formation is interpreted to have involved melting of upwelling mantle with cyclical eruption, burial and partial melting of basaltic crust yielding multiple generations of TTGs and granites in the interval 3.53–3.24 Ga, leading

to the development of a thick continental lithosphere underlain by melt-depleted residual mantle (Smithies et al., 2005, 2009; Van Kranendonk et al., 2007). Similar dome-and-keel structures are reproduced within our reference experiment, where felsic rocks produced from mafic crust during mantle-upwelling–crustal delamination events are intruded into the overlying mafic crust (see Fig. 2f,g and Movie 1). Such long-term intracrustal recycling is widely supported by the Archean zircon record (e.g. Kemp et al., 2010; Zeh et al., 2009, 2013).

By contrast, the Archean of West Greenland consists of orthogneisses with a subordinate amount of highly deformed greenstones and anorthosite–gabbro intrusions (e.g. Nutman et al., 2007, 2013). The gneisses have been interpreted to represent a collage of terranes with distinct ages and internal evolution that are separated from each other by mylonite zones (e.g. Nutman et al., 1989, 2007, 2013; Van Kranendonk, 2010). This type of crustal collage has been argued to have formed by shallow subduction and crustal imbrication during collisional orogenesis and subsequent crustal thinning (Nutman et al., 2009, 2013). The results of our reference experiment suggest intriguing similarities with the model proposed for the Archean of West Greenland by Nutman et al. (2009, 2013). For example, the progressive shortening induced by the cyclically-opening spreading center on the left side of the model leads to shortening and thickening of the initial granite-greenstone crust, and finally a short-lived subduction event. Reworking of the crust by sagduction of the dry basalt (gabbro) intrusions separating the blocks of granite-greenstone crust (Fig. 2h), leads to a dominantly felsic crust, while the later short-lived subduction event could be responsible for subsequent crustal thinning similar to that in the Archean of West Greenland.

Thus, our geodynamic experiments demonstrates the possible development of granite–greenstone terranes by vertical tectonics related to mantle upwelling and the development of felsic gneiss terranes by horizontal tectonics related to spreading and subduction. In the reference experiment these two types of crust were developed sequentially rather than contemporaneously, which is in a good agreement with a number of transitional terrains in the Archean showing intermediate characteristics (Windley and Bridgwater, 1971). Indeed, the reference experiment shows a temporal transition from vertical to horizontal tectonics related to the development of cyclic spreading as the experiment progressed and, ultimately, the occurrence of a brief period of subduction. There is ample evidence of crustal shortening recorded in granite–greenstone terranes (Bickle et al., 1980; Kröner, 1991; Kröner and Layer, 1992; Park, 1981). In our experiment, crustal shortening evidence within granite–greenstone like crust is either related to the cycle of delamination events and consequent mantle upwelling, or related to the lateral advancement of an oceanic-type plate. It is the lateral advance of the oceanic-type plate that is partly responsible for the continuous rise of the dacite domes that initially form during the delamination–mantle upwelling events (Movie 1).

Lastly, vertical accretion through magmatic underplating has been considered to be an important process on Earth (e.g. Cox, 1993; Thybo and Artemieva, 2013) and might have been a more dominant process in the formation of the continental-like crust on early Earth (e.g. Kröner, 1991; Kröner and Layer, 1992). Also, delamination of the cumulate products of underplated mafic igneous complexes or their eclogitized equivalents (Cox, 1993; Thybo and Artemieva, 2013) might also be a major process that operated in the Archean. These processes could have generated a cycle of underplating and delamination. During such a cycle, melt and heat are provided to the base of the crust at the new Moho created by the delamination event as a result of asthenospheric upwelling and decompression melting, which, in turn, was triggered by the delamination event (e.g. Anderson, 2005; Hamilton, 2007).

4.3. Mechanisms for the formation of felsic crust

Although the formation of Archean TTGs by melting of hydrated basalts at garnet-amphibolite, granulite or eclogite facies was established based on geochemistry and confirmed by experiments (e.g. Moyen and Martin, 2012, and references therein), the relationship to one or another geodynamic setting is more debatable. The three groups of TTGs defined by Moyen (2011) are not discrete, but show continuous chemical variation from the low to the high pressure group, suggesting a common source but variable depth of melting. The pressure range for melting hydrated basalt in our experiments (Fig. 3) covers the full range identified by Moyen (2011). Within the reference experiment, melting of hydrated enriched basalt to produce dacitic melts occurs during dripping of the lower crust and small-scale crustal overturns, with a variation in pressure from ~0.5 to >2.0 GPa, and within the crust, mostly around 1.0 GPa. Melting in these different tectonic settings may occur simultaneously.

The results of our petrological-thermomechanical tectonomagmatic modeling conflict with paradigm of uniformitarianism, which remains a strong tenet in interpretations of the Archean crustal record (e.g. Cawood et al., 2006; Kerrich and Polat, 2006; Polat et al., 2009, and references therein). For example, greenstone belts are commonly interpreted as related to oceanic arcs or oceanic plateaus, or as collages of oceanic arcs, plateaus and subduction-accretion complexes (e.g. Kimura et al., 1993; Polat et al., 1998; Puchtel et al., 1998). Furthermore, based on comparisons with rare exotic volcanic rocks in Cenozoic arcs, Archean boninites and picrites have been related to hot subduction in a mobilist Archean geodynamic regime (Polat and Kerrich, 2006).

A model based on slab melting at subduction zones was predicated on an assumption of subducting young, hot oceanic lithosphere to provide the extensive degree of melting required to satisfy the volume of TTG magmas represented by the Archean crust (e.g. Arth and Hanson, 1975; Condie, 1981; Martin, 1986; Martin and Moyen, 2002). That is not supported by our modeling. In the reference experiment, the strongly depleted heterogeneous oceanic-type lithospheric plate, which is adjacent to the continental-type crustal domain, is rather old (c. 100 Ma) and too cold to be significantly melted during subduction (e.g. Fig. 2j–o), although over the period of subduction younger and hotter lithosphere is progressively involved in the process. Whatever the case, in the experiment the subducting plate comprises MORB-like oceanic crust, which is unlikely to produce the arc-like signature of Archean TTGs (Martin et al., 2014). In addition, an alternative proposition involving subduction of an oceanic plateau (Martin et al., 2014) is not supported by our modeling. On the other hand, the rationale behind the Martin et al. (2014) model is the requirement of an enriched mantle source for TTG magmas, which is met in our modeling. Furthermore, it has been suggested that an arc-like signature similar to that produced by subduction can be a result of partial melting of hydrated mafic crust during delamination (Moyen and Martin, 2012), as discussed below.

In our experiments, both delamination and small-scale crustal overturns may lead to interaction between dacitic melts extracted from the hydrated basalt and the complementary upwelling hot melt-bearing mantle. The small-scale crustal overturns represent an alternative setting to subduction for the production of high-to-medium pressure TTGs, since the right source (hydrated basalt) occurs at the right depth (>1.2 GPa). Indeed, the small-scale crustal overturns would produce mostly medium-pressure TTG melts, which strongly prevail over the low- and high-pressure TTGs within Archean terranes (Moyen, 2011). However, the volume of TTGs comprising the Archean crust likely requires that the small-scale crustal overturns occur more frequently in the Archean than observed in the reference experiment. Since the appearance of the

small-scale crustal overturns is strongly linked to the production of mantle-derived melts, an increase of upper-mantle temperature or radiogenic heat production (experiments try83 and try55 in Table 2) lead to more vigorous crustal overturns and a higher volume of production of TTG melts.

While the medium- and high-pressure TTGs might be produced by crustal overturns and delamination, respectively, melting of the locally thickened or/and locally heated crust (at 30–40 km depth, Fig. 3b) could lead to the production of low pressure TTGs, as has been suggested by Qian and Hermann (2013) and Zhang et al. (2013) based on melting experiments. In our experiment, the thickened oceanic-type crust forms due to melting of hot ambient mantle, and not by hot mantle plumes as was suggested by Smithies et al. (2009). The formation of the Krossfjordur dacites in Iceland (Willbold et al., 2009) may be a modern analog of melting at the base of mafic crust in the Archean. This example demonstrates the possibility of an intra-plate origin for TTG-like magmas by melting the lower portion of a mafic crust (amphibolite) driven by heat from underplated mantle-derived melts.

4.4. Comparison with other numerical models

This study has identified an interchange between a stagnant-deformable lid regime with predominantly vertical tectonics processes and periods of horizontal tectonic activity leading to short-lived episodes of subduction (Fig. 2). Each of these regimes imposes a distinctive structure on the continental crust, via the formation of granite-greenstone crust and its subsequent reworking, respectively. The diversity of geochemical characteristics of the Archean crust has led to conflicting tectonic scenarios being proposed for the Archean, either related to a stagnant-lid or a mobile-lid tectonic regime. Our study supports the proposed models of episodic subduction in the Archean (e.g. Debaillé et al., 2013; Moyen and Van Hunen, 2012; O'Neill et al., 2007a,b). In the majority of such models pulses of rapid subduction are assumed to result in massive arc volcanism and continental growth by arc-accretion.

However, in our reference experiment, magmatic activity during subduction is mostly related to the partial melting of the sedimentary rocks during subduction and the generation of dry basaltic melts by the mantle upwelling beneath the backarc zone, whereas the magmatism responsible for intracrustal differentiation and maturation of the continental-like crust is mostly generated during the dominantly stagnant-deformable lid regime of vertical tectonics and tectono-magmatic crust-mantle interactions (Fig. 2a–h). Subduction is initiated spontaneously due to the mantle convection-driven advance of the oceanic-type lithospheric plate from the left and the rise of felsic diapirs within the shortened continental-type lithospheric plate (Fig. 2). After initiation, subduction is maintained mainly by eclogitization of basalt within the thick mafic crust, causing the slab to retreat with subsequent stretching of the continental-type plate and opening of a backarc-like extension region in the thinned continental-like crust. This contrasts with the experiment by Rey et al. (2014) for a mantle 200 K hotter than at present, where transient episodes of plate tectonics were initiated by the high gravitationally-generated horizontal stress between a prescribed thick continental lithosphere and a thinner oceanic plate. The high stress drives collapse of the continental lithosphere, which thins from ~225 km to ~75 km thick on average, provoking the adjacent oceanic plate to subduct.

The results of our experiments demonstrate the dominant role of delamination–mantle upwelling events for the formation of granite-greenstone crust with dome-and-keel geometry. During these delamination–mantle upwelling events, TTG melts are generated from basalt by melting due to the intrusion of mantle-derived hot dry basaltic melts. This process is consistent with the initial idea of sagduction proposed by Goodwin and Smith (1980) and with the

more recent model of Bédard (2006), who argued that a combination of mantle diaps with delamination of crustal residues could give rise to the multistage formation of TTG melts generated in the deeper portions of oceanic plateaus. However, in comparison with the cold crust implied for the Archean by the purely volcanic magmatic accretion model (volcanic heat-pipe model) of Moore and Webb (2013), the crust in our more realistic volcanic-plutonic magmatic accretion model (volcanic-plutonic heat-pipe model) is rather hot, which enables both the hot crustal temperatures and the longevity of coupled magmatic and tectonic activity necessary to explain the geological record of the Archean crust.

4.5. Formation of the sub-continental lithospheric mantle (SCLM)

The higher mantle potential temperatures in the Archean must correspond to a greater extent of mantle melting. The melt fractions derived from cratonic peridotites are estimated to have been 0.25–0.45, at initial melting pressures of 3–6 GPa (Herzberg et al., 2010). Indeed, the Archean SCLM is rather thick (150–200 km or more), consistent with this observation, and consists mostly of depleted peridotite (harzburgite), which is interpreted as the residue from the production of primary melts of the dominant non-arc basalts found in greenstone belts (Herzberg and Rudnick, 2012). However, the age of the SCLM appears to be rather young—predominantly Mesoarchean to Neoarchean (Griffin et al., 2013; Pearson and Wittig, 2008). This is consistent with results of our modeling as well as that of others (e.g. Griffin et al., 2013; Johnson et al., 2014), which generally shows that the early mantle residues are recycled due to the vigorous convection in a hotter mantle, and that the internally convecting SCLM only becomes stabilized as the mantle cools.

Pb and Hf isotope data from detrital zircons from the Jack Hills metasedimentary belt, and from zircons in the neighboring Paleoarchean-to-Mesoarchean Narrabeen gneisses and Neoarchean granites in Western Australia indicate an evolution consistent with protracted intracrustal reworking of an enriched, dominantly mafic protolith that was extracted from the mantle in the Hadean (Kemp et al., 2010). However, there is no evidence in this region for the existence of strongly depleted Hadean mantle. By contrast there is some Nd isotope evidence from the earliest known crustal rocks from West Greenland, up to c. 3.8 Ga in age, that suggests the possibility that an initial chondritic mantle could have been depleted by the Eoarchean (Jacobsen and Dymek, 1988). Whatever the case for the Earth as a whole, it is clear that the earliest-formed crust is older than the average age of the stable SCLM.

The depleted lithospheric mantle in our reference experiment forms initially during the intensive delamination–mantle upwelling events. During this process, the depleted peridotite mixes with the rising fertile peridotite, while the lower crust, represented by the residues of dry basalt partial melting, cumulates after fractional crystallization of dry basaltic melts, and eclogites formed during ongoing burial of the crust, becomes denser than underlying peridotite and delaminates. Based on high-pressure experiments on compositions similar to these partial melting residues, Tatsumi et al. (2014) proposed that they might sink to the core–mantle boundary, forming “anti-continents”. The depleted positively buoyant SCLM remains in a suprasolidus internally convecting state throughout the experiment. By contrast, Bédard (2006) argued that the delaminating eclogite should have refertilized the depleted mantle. In turn, the refertilized mantle could have yielded additional melt, leaving behind the most severely depleted mantle (e.g. Griffin et al., 2003).

In a stagnant-deformable lid tectonic regime, the lithospheric delamination–mantle upwelling events do not mix the mantle well (Fig. 6c). Indeed, the lack of horizontal plate movement during the periods of stagnant-deformable lid behavior stabilizes the

convective cells and minimizes lateral mixing of materials between the cells (Schmalzl et al., 1996). Once the oceanic-type plate is able to advance, the mantle underneath the continental-type plate starts to mix laterally as well as vertically, reducing the lateral heterogeneity (Fig. 6d,e). After c. 100 Ma this process leads to the formation of a rather thick (~180 km), and well-mixed depleted SCLM with an average melt depletion of 0.25–0.3 (see Fig. 6d,e). This is consistent with the hot regime and intensive convection expected in the Archean mantle, which results in efficient mixing and homogenization in less than 100 Ma (e.g. Coltice and Schmalzl, 2006; Van Keken and Zhong, 1999). The strongly depleted lithospheric mantle of oceanic-like domains is also involved in subduction, which causes the rise of more fertile mantle beneath the continental-type plate after the slab breakoff (Fig. 6f). After the transition to a mobile-lid tectonic regime, the depleted lithospheric mantle, which was homogenized during the stagnant-deformable lid tectonic regime, undergoes some redistribution due to partial involvement in the subduction and mixing with more fertile mantle. In addition, the lithospheric mantle may be modified by interactions with melt and/or fluid derived from the subducting oceanic-type plate.

The model described above, which is based on the results of our experiments, is similar to that proposed by Herzberg and Rudnick (2012) for the formation of cratonic lithosphere. These authors note that cratonization of the continental crust occurred largely in the interval 3.5–2.5 Ga, when ambient mantle was hot and extensive melting would have produced a primary ultramafic–mafic crust ~30–45 km thick. Herzberg and Rudnick (2012) used the absence of much of this primary crust compared to the craton-wide distribution of harzburgite residues to argue for its loss via foundering of the lithosphere. Furthermore, they proposed that the foundering primary crust would have partially melted to produce the TTGs required for the formation of continental crust, similar to the results of our experiment. In their model, Herzberg and Rudnick (2012) posit that the remaining lithosphere would have gravitationally separated into residual eclogite, which would have continued to sink, and buoyant harzburgite, which would have returned by buoyancy-driven diapirism to underplate the cratonic nuclei composed of TTG crust and overlying non-arc basalts. Indeed, our experiments suggest that some of the deeply subducted/delaminated chemically buoyant depleted mantle may actually separate from the associated dense eclogite, rise back and re-accrete to SCLM at much later stages after long period of residence and heating in the deep mantle (Fig. 6). As the reference experiment evolved, so the SCLM developed contemporaneously with the initiation of the episodic subduction events. Finally, Herzberg and Rudnick (2012) propose that during the assembly of cratonic nuclei into cratons by subduction, the harzburgite residues would have been substantially modified by melt–rock interactions. This final stage would be consistent with the transition from a stagnant-deformable lid tectonic regime to a mobile-lid tectonic regime.

4.6. The accretionary complex in the trench

Toward the end of the reference experiment, subduction initiated and a very large accretionary complex developed in the trench (Fig. 2i) due to the prescribed high rate of sedimentation in the steeply dipping trench area. The sedimentary rocks that preferentially accumulated in the trench were subducted with the oceanic plate and undergo partial melting before exhumation. The sedimentary rocks of the accretionary complex create an increase in buoyancy of the subducting material, which competes with an increase in the density of the slab due to the conversion of the thick basaltic crust to eclogite. Eventually, the increased buoyancy leads to the transitional dripping off (or breakoff) behavior of the slab (Fig. 2i,l) and the termination of subduction (Fig. 2k,n).

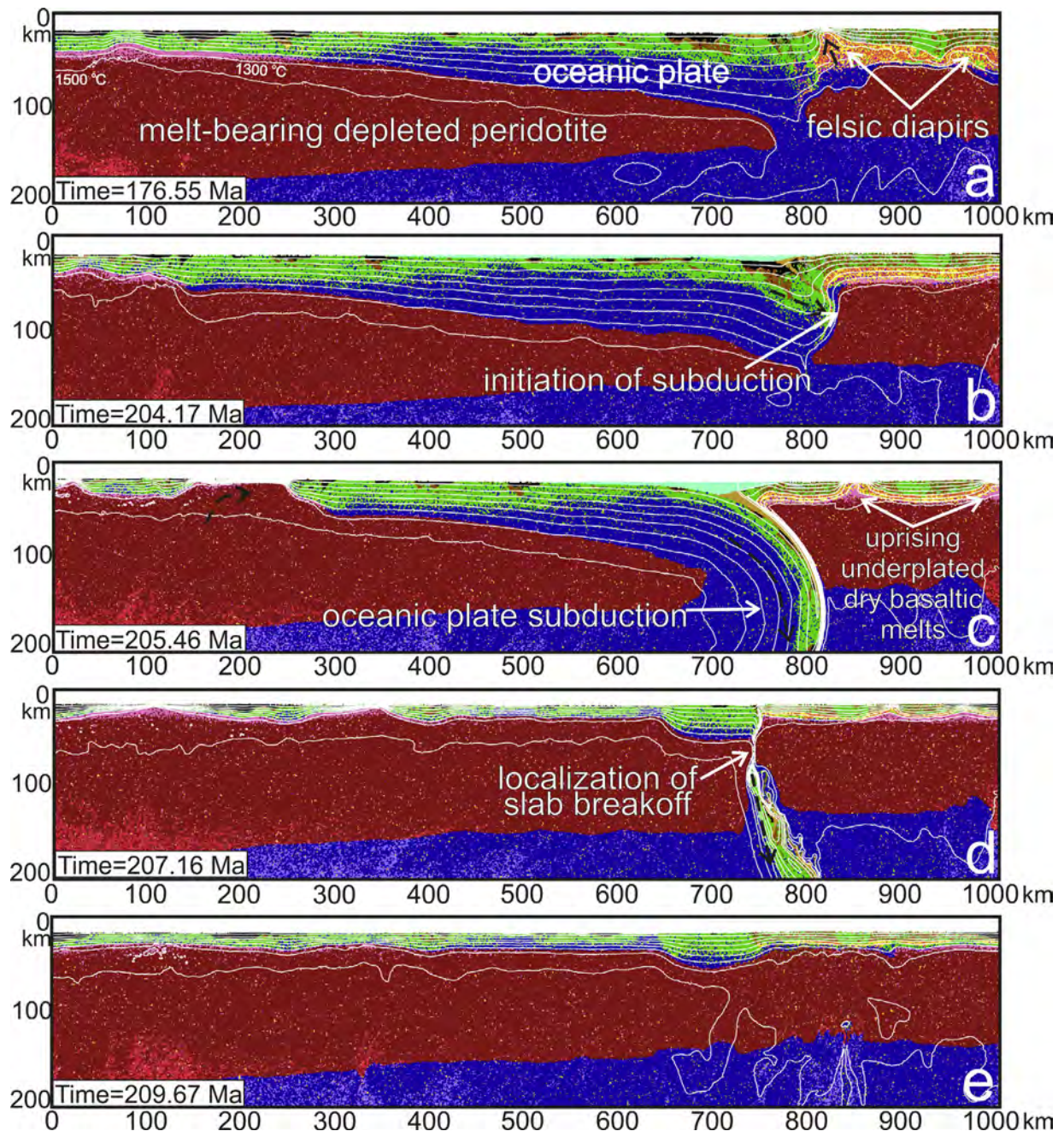


Fig. 10. Representative time-slice snapshots to show an alternative evolution of the final stage of the reference experiment with a revised parametrization for the sedimentation process (see Section 4.6 for details). The modified experiment starts with the felsic diapirs rising within the continental-like crust (cf. a and Fig. 2h). The oceanic-type lithospheric plate slowly moves to the right as a result of the upwelling mantle, and eventually underthrusts the continental-like crust (b). After the transition of the frontal part of the oceanic crust to eclogite the oceanic-type plate spontaneously subducts to the right beneath the continental-type plate (c). The subduction is terminated by slab breakoff (d), and the tectonic regime reverts to a stagnant-lid (e).

To limit the buoyancy effect of the very large accretionary complex, the final stage of the experiment was repeated with a revised parametrization for the sedimentation process. In particular, the sediments were not allowed to accumulate in the trench beyond a depth limit, which decreased the volume of sedimentary rocks available to be dragged down by subduction. This modified experiment developed a single episode of subduction during the final stage (Fig. 10). In this case, the felsic diapirs do not provoke subduction (cf. Figs. 2h and 10a). Instead, the oceanic-like plate slowly moves to the right as a result of the upwelling mantle drag and push, and eventually underthrusts the more buoyant continental-like crust (Fig. 10b). As soon as the thick oceanic crust starts to transform

to eclogite, the oceanic-like plate spontaneously subducts to the right beneath the continental-type plate (Fig. 10c). The trench retreat that is generated by the subduction process causes decompression melting of the mantle beneath the continental-type plate and thinning of the continental crust from ~50 km to ~20 km on average (Fig. 10c). After 3 Ma, the subduction is terminated by slab breakoff (Fig. 10d), and the tectonic regime reverts to a stagnant-deformable lid (Fig. 10e).

In both of these experiments, the horizontal tectonic processes are terminated by a short-lived subduction event. The differences between the two experiments relate to (1) the type of subduction, either continuous (without the involvement of a large accretionary

complex) or interrupted (with an artificially large accretionary complex), and (2) the effect of the accretionary complex on the overlying continental-type plate, which is strongly reworked by magmatism in the experiment with the large accretionary complex. Since the subduction is rather short-lived and steep in both experiments, melting of the subducting oceanic crust is largely precluded. Thus, there is no subduction related episode of crustal growth, in contrast to the experiments of Moyen and Van Hunen (2012). Nevertheless, the evolution of our experiments is in a good agreement with the consensus for the Eoarchean–Mesoarchean of a dominantly stagnant-deformable lid tectonic regime with episodic subduction (e.g. O'Neill and Debaille, 2014).

5. Conclusions

Results of the 2D petrological–thermomechanical tectono-magmatic numerical experiments developed for conditions appropriate to the hotter early Archean lithosphere demonstrate a variety of tectono-magmatic settings in which felsic melts can be generated from hydrated primitive basaltic crust: (1) delamination and dripping of the lower primitive basaltic crust into the mantle; (2) local thickening of the primitive basaltic crust; and (3) small-scale crustal overturns. Based on the P - T conditions in the experiments, many of the melts produced from the hydrated basalt during small-scale crustal overturns or lower crustal delamination likely correspond to the prevalent Archean TTG suites, while other melts could cover the remaining diversity of Archean granitoids. In the context of a stagnant-deformable lid tectonic regime that is intermittently terminated by short-lived subduction, we identify the sequential development of two distinct types of continental-like crust. The early type of continental-like crust is composed of TTGs and greenstones with dome-and-keel geometry formed from the original thick basaltic crust that was reworked into a more felsic crust by the processes of delamination, melting, magmatism and deformation occurring over delaminating-upwelling mantle. By contrast, the second type of continental-like crust represents tectonic reworking of accreted material comprising strongly deformed granite–greenstone and subduction-related sequences. The intensive crustal shortening and thickening results in preservation of the felsic material as the mafic material is lost by dripping into the mantle. Thus, a regime of dominantly vertical tectonics is followed by a regime in which both horizontal and vertical tectonics occurs. The results of our reference experiment are in a good agreement with the consensus that the Archean might have been dominated by a stagnant-lid tectonic regime with the possibility of episodic transient subduction and mobile-lid tectonics. Thus, we have provided a conceptual framework for separating different types of continental crust according to the likely tectonic regime.

Finally, we stress the tectono-magmatic character of the crust–mantle interactions leading to formation of TTG. We conclude that melting-induced crustal convection, lithospheric delamination, the formation of eclogitic drips and the growth of a positively buoyant internally-convection depleted subcontinental mantle layer are essential processes responsible for the formation of Archean cratons.

Acknowledgments

We acknowledge the two journal reviewers, J.F. Moyen and C. Herzberg, for detailed comments that helped us improve the paper during revision. This work was supported by Austrian Science Fund (FWF), Lise Meitner Program, project number M 1559-N29 (E.S.) and by an ETH-grant ETH-37.11-2 (T.G.). Simulations were performed on the ETH-Zurich Brutus cluster.

Appendix A. Supplementary data

Supplementary material related to this article can be found, in the online version, at <http://dx.doi.org/10.1016/j.precamres.2015.10.005>.

References

- Abbott, D., Burgess, L., Longhi, J., Smith, W.H.F., 1994. An empirical thermal history of the Earth's upper mantle. *J. Geophys. Res.* 99, 13835–13850.
- Anderson, D.L., 2005. Large igneous provinces, delamination, and fertile mantle. *Elements* 1, 271–275.
- Arth, J.G., Hanson, G.N., 1975. Geochemistry and origin of the Early Precambrian crust of north-eastern Minnesota. *Geochim. Cosmochim. Acta* 39, 325–362.
- Arth, J.G., Barker, F., Peterman, Z.E., Frideman, I., 1978. Geochemistry of the gabbro–diorite–tonalite–trondhjemite suite of south-west Finland and its implications for the origin of tonalitic and trondhjemitic magmas. *J. Petrol.* 19, 289–316.
- Atherton, N.P., Petford, N., 1993. Generation of sodium-rich magmas from newly underplated basaltic crust. *Nature* 362, 144–146.
- Barker, F., Arth, J.G., 1976. Generation of trondhjemite–tonalite liquids and Archaean bimodal trondhjemite–basalt suites. *Geology* 4, 596–600.
- Benn, K., Moyen, J.-F., 2008. Geodynamic origin and tectonomagmatic evolution of the late Archean abitibi–opatica terrane, Superior Province: magmatic modification of a plateau-type crust and plume–subduction interaction. In: Condie, K.C., Pease, V. (Eds.), When did Plate Tectonics Begin on Earth? Geological Society of America Special Paper, 440, 173–198.
- Bédard, J.H., 2006. A catalytic delamination-driven model for coupled genesis of Archaean crust and sub-continental lithospheric mantle. *Geochim. Cosmochim. Acta* 70, 1188–1214.
- Bédard, J.H., Harris, L.B., 2014. Neorachean disaggregation and reassembly of the Superior craton. *Geology* 42, 951–954.
- Bédard, J.H., Harris, L.B., Thruston, P.C., 2013. The hunting of the snArc. *Precambrian Res.* 229, 20–48.
- Bickle, M.J., 1978. Heat loss from the Earth: a constraint on Archean tectonics from the relation between geothermal gradients and the rate of plate production. *Earth Planet. Sci. Lett.* 40, 301–315.
- Bickle, M.J., Bettenay, L.F., Boulter, C.A., Groves, D.I., Morant, P., 1980. Horizontal tectonic interaction of an Archean gneiss belt and greenstones, Pilbara block, Western Australia. *Geology* 8, 525–529.
- Bittner, D., Schmelting, H., 1995. Numerical modelling of melting processes and induced diapirism in the lower crust. *Geophys. J. Int.* 123, 59–70.
- Brown, M., 2007. Metamorphic conditions in orogenic belts: a record of secular change. *Int. Geol. Rev.* 49 (3), 193–234.
- Brown, M., 2014. The contribution of metamorphic petrology to understanding lithosphere evolution and geodynamics. *Geosci. Front.* 5, 553–569.
- Carmichael, I.S.E., 1964. The petrology of Thingmuli, a tertiary volcano in eastern Iceland. *J. Petrol.* 5 (3), 435–460.
- Cawood, A.P., Kröner, A., Pisarevsky, S., 2006. Precambrian plate tectonics: criteria and evidence. *Geol. Soc. Am. Today* 16, 4–11.
- Coltice, N., Schmalzl, J., 2006. Mixing times in the mantle of the early Earth derived from 2-D and 3-D numerical simulations of convection. *Geophys. Res. Lett.* 33, L23304, <http://dx.doi.org/10.1029/2006GL027707>.
- Condie, K.C., 1981. Archean Greenstone Belts. Elsevier, Amsterdam.
- Condie, K.C., 1986. Origin and early growth rate of continents. *Precambrian Res.* 32, 261–278.
- Cox, K.G., 1993. Continental magmatic underplating. *Philos. Trans. R. Soc. Lond.* 342, 155–166.
- Crisp, J.A., 1984. Rates of magma emplacement and volcanic output. *J. Volcanol. Geotherm. Res.* 20, 177–211.
- Cutts, C.A., Stevens, G., Hoffmann, J.E., Buick, I.S., Frei, D., Münker, C., 2014. Paleo-to Mesoarchean polymetamorphism in the Barberton Granite–Greenstone Belt, South Africa: constraints from U–Pb monazite and Lu–Hf garnet geochronology on the tectonic processes that shaped the belt. *Geol. Soc. Am. Bull.* 126, 251–270.
- Davies, G.F., 1992. On the emergence of plate-tectonics. *Geology* 20 (11), 963–966.
- Debaille, V., O'Neill, C., Brandon, A.D., Haenecour, P., Yin, Q.-Z., Mattielli, N., Treiman, A.H., 2013. *Earth Planet. Sci. Lett.* 373, 83–92.
- Dhuime, B., Hawkesworth, C.J., Cawood, P.A., Storey, C.D., 2012. A change in the geodynamics of continental growth 3 billion years ago. *Science* 335, 1334–1336.
- Djomani, Y.H.P., O'Reilly, S.Y., Griffin, W.L., Morgan, P., 2001. The density structure of subcontinental lithosphere through time. *Earth Planet. Sci. Lett.* 184, 605–621.
- Foley, S., Tiepolo, M., Vannucci, R., 2002. Growth of early continental crust controlled by melting of amphibolite in subduction zones. *Nature* 417, 837–840.
- Foley, S.F., Buhre, S., Jacob, D.E., 2003. Evolution of the Archean crust by delamination and shallow subduction. *Nature* 421, 249–252.
- François, C., Philippot, P., Rey, P., Rubatto, D., 2014. Burial and exhumation during Archean sagduction in the East Pilbara Granite–Greenstone Terrane. *Earth Planet. Sci. Lett.* 396, 235–251.
- Gerya, T.V., Yuen, D.A., 2003a. Characteristics-basedmarker-in-cellmethod with conservative finite-differences schemes for modelling geological flows with strongly variable transport properties. *Phys. Earth Planet. Inter.* 140, 295–318.
- Gerya, T.V., Yuen, D.A., 2003b. Rayleigh–Taylor instabilities from hydration and melting propelling “cold plumes” at subduction zones. *Earth Planet. Sci. Lett.* 212, 47–62.

- Gerya, T.V., Yuen, D.A., 2007. Robust characteristics method for modelling multiphase visco-elasto-plastic thermo-mechanical problems. *Phys. Earth Planet. Inter.* 163, 83–105.
- Goodwin, A.M., 1991. *Precambrian Geology*. Academic Press, pp. 666.
- Goodwin, A.M., Smith, I.E.M., 1980. Chemical discontinuities in Archean metavolcanic terrains and the development of Archean crust. *Precambrian Res.* 10, 301–311.
- Griffin, W.L., O'Reilly, S.Y., Abe, N., Aulbach, S., Davies, R.M., Pearson, N.J., Doyle, B.J., Kivi, K., 2003. The origin and evolution of Archean lithospheric mantle. *Precambrian Res.* 127, 19–41.
- Griffin, W.L., Belousova, E.A., O'Neill, C., O'Reilly, Suzanne, Y., Malkovets, V., Pearson, N.J., Spetsius, S., Wilde, S.A., 2013. The world turns over: Hadean–Archean crust–mantle evolution. *Lithos* 189, 2–15.
- Grove, T.L., Elkins, L.T., Parman, S.W., Chatterjee, N., Müntener, O., Gaetani, G.A., 2003. Fractional crystallization and mantle-melting controls on calc-alkaline differentiation trends. *Contrib. Mineral. Petrol.* 145, 515–533.
- Hacker, B.R., Abers, G.A., Peacock, S.M., 2003. Subduction factory: 1. Theoretical mineralogy, densities, seismic wave speeds, and H₂O contents. *J. Geophys. Res.* 108 (B1), 2029, <http://dx.doi.org/10.1029/2001JB001127>.
- Hamilton, W.B., 2007. Earth's first two billion years—the era of internally mobile crust. *Geol. Soc. Am. Mem.* 200, 233–296.
- Hastie, A.R., Fitton, J.G., Mitchell, S.F., Neill, I., Nowell, G.M., Millar, I.L., 2015. Can fractional crystallization, mixing and assimilation processes be responsible for Jamaican-type Adakites? Implications for generating eoarchean continental crust. *J. Petrol.*, <http://dx.doi.org/10.1093/petrology/egv029> (published online July 29, 2015).
- Herzberg, C., Asimow, P.D., Arndt, N., Niu, Y., Lesher, C.M., Fitton, J.G., Cheadle, M.J., Saunders, A.D., 2007. Temperatures in ambient mantle and plumes: constraints from basalts, picrites and komatiites. *Geochem. Geophys. Geosyst.* 8, Q02006.
- Herzberg, C., Condie, K., Korenaga, J., 2010. Thermal history of the Earth and its petrological expression. *Earth Planet. Sci. Lett.* 292, 79–88.
- Herzberg, C., Rudnick, R., 2012. Formation of cratonic lithosphere: an integrated thermal and petrological model. *Lithos* 149, 4–15.
- Ito, K., Kennedy, G.C., 2013. An experimental study of the basalt-garnet granulite-eclogite transition. In: Heacock, J.G. (Ed.), *The Structure and Physical Properties of the Earth's Crust*. American Geophysical Union, Washington, DC, <http://dx.doi.org/10.1029/GM014p0303>.
- Jacobsen, S.B., Dymek, R.F., 1988. Nd and Sr isotope systematics of clastic metasediments from Isua, West Greenland: identification of Pre-3.8 Ga differentiated crustal components. *J. Geophys. Res.* 93, 338–354.
- Jagoutz, O., Schmidt, M.W., Enggist, A., Burg, J.-P., Hamid, D., Hussain, S., 2013. TTG-type plutonic rocks formed in a modern arc batholith by hydrous fractionation in the lower arc crust. *Contrib. Mineral. Petrol.* 166, 1099–1118.
- Jahn, B.M., Glikson, A.Y., Peucat, J.-J., Hickman, A.H., 1981. REE geochemistry and isotopic data of Archean silicic volcanics and granitoids from the Pilbara Block, western Australia: implications for the early crustal evolution. *Geochim. Cosmochim. Acta* 45, 1633–1652.
- Johnson, T.E., Brown, M., Kaus, B., Van Tongeren, J.A., 2014. Delamination and recycling of Archean crust caused by gravitational instabilities. *Nat. Geosci.* 7, 47–52.
- Jordan, T.H., 1978. Composition and development of the continental tectosphere. *Nature* 274, 544–548.
- Kamo, S.L., Davis, D.W., 1994. Reassessment of Archean crustal development in the Barberton Mountain Land, South Africa, based on U-Pb dating. *Tectonics* 13, 167–192.
- Katz, R.F., Spiegelman, M., Langmuir, C.H., 2003. A new parameterization of hydrous mantle melting. *Geochem. Geophys. Geosyst.* 4 (9), 1073, <http://dx.doi.org/10.1029/2002GC000433>.
- Keller, C.B., Schoene, B., 2012. Statistical geochemistry reveals disruption in secular lithospheric evolution about 2.5 Gyr ago. *Nature* 485, 490–493.
- Kemp, A.I.S., Wilde, S.A., Hawkesworth, C.J., Coath, C.D., Nemchin, A., Pidgeon, R.T., Vervoort, J.D., DuFrane, S.A., 2010. Hadean crustal evolution revisited: new constraints from Pb-Hf isotope systematics of the Jack Hills zircons. *Earth Planet. Sci. Lett.* 296, 45–56.
- Kerrich, R., Polat, A., 2006. Archean greenstone-tonalite duality: thermochemical mantle convection models or plate tectonics in the early Earth global dynamics? *Tectonophysics* 415, 141–165.
- Kimura, G., Ludden, J.N., Desrochers, J.-P., Hori, R., 1993. A model of ocean–crust accretion for the Superior Province, Canada. *Lithos* 30, 337–355.
- Kleinmanns, I.C., Kramers, J.D., Kammer, B.S., 2003. Importance of water for Archean granitoid petrology: a comparative study of TTG and potassic granitoids from Barberton Mountain Land, South Africa. *Contrib. Mineral. Petrol.* 145, 377–389.
- Korenaga, J., 2008a. Plate tectonics, flood basalts, and the evolution of Earth's oceans. *Terra Nova* 20, 419–439.
- Korenaga, J., 2008b. Urey ratio and the structure and evolution of Earth's mantle. *Rev. Geophys.* 46, RG2007, <http://dx.doi.org/10.1029/2007RG000241>.
- Kröner, A., 1991. Tectonic evolution in the Archean and Proterozoic. *Tectonophysics* 187, 393–410.
- Kröner, A., Layer, P., 1992. Crust formation and plate motion in the early Archean. *Science* 256, 1405.
- Labrosse, S., Jaupart, C., 2007. Thermal evolution of the Earth: secular changes and fluctuations of plate characteristics. *Earth Planet. Sci. Lett.* 260, 465–481.
- Laurent, O., Martin, H., Moyen, J.-F., Doucelance, R., 2014. The diversity and evolution of late-Archean granitoids: evidence for the onset of "modern-style" plate tectonics between 3.0 and 2.5 Ga. *Lithos* 205, 208–235.
- Martin, H., 1986. Effect of steeper Archean geothermal gradient on geochemistry of subduction zone magmas. *Geology* 14, 753–756.
- Martin, H., Moyen, J.-F., 2002. Secular changes in TTG composition as markers of the progressive cooling of the Earth. *Geology* 30 (4), 319–322.
- Martin, H., Smithies, R., Rapp, R.P., Moyen, J.F., Champion, D., 2005. An overview of adakite, TTG, and sanukitoid: relationships and some implications for crustal evolution. *Lithos* 79, 1–24.
- Martin, H., Moyen, J.-F., Guitreau, M., Blichert-Toft, J., Le Pennec, J.-L., 2014. Why Archean TTG cannot be generated by MORB melting in subduction zones. *Lithos* 198–199, 1–13.
- Moore, W.B., Webb, A.A.G., 2013. Heat-pipe Earth. *Nature* 501, 501–505.
- Moresi, L., Solomatov, V.S., 1998. Mantle convection with a brittle lithosphere: thoughts on the global tectonic styles of the Earth and Venus. *Geophys. J. Int.* 133, 669–682.
- Moyen, J.-F., 2011. The composite Archean grey gneisses: petrological significance, and evidence for a non-unique tectonic setting for Archean crustal growth. *Lithos* 123, 21–36.
- Moyen, J.-F., Martin, H., 2012. Forty years of TTG research. *Lithos* 148, 312–336.
- Moyen, J.-F., Stevens, G., 2004. Evolution of TTG Geochemistry around the Barberton Greenstone Belt from 3.5 to 3.2 Ga: Transition from Shallow Melting below Under-plated Crust to Subduction-Associated Magmatism? *Geocongress, Johannesburg (South Africa)*.
- Moyen, J.-F., Stevens, G., 2006. Experimental constraints on TTG petrogenesis: implications for Archean geodynamics. In: Benn, K., Mareschal, J.-C., Condie, K.C. (Eds.), *Archean Geodynamics and Environments*. AGU, pp. 149–178.
- Moyen, J.-F., Van Hunen, J., 2012. Short-term episodicity of Archean plate tectonics. *Geology* 40 (5), 451–454.
- Moyen, J.-F., Stevens, G., Kisters, A.F.M., 2006. Record of mid-Archean subduction from metamorphism in the Barberton terrain, South Africa. *Nature* 442, 559–562.
- Moyen, J.-F., Stevens, G., Kisters, A.F.M., Belcher, R.W., Chapter 5 2007. 6 TTG Plutons of the Barberton Granitoid–Greenstone Terrain, South Africa. *Earth's oldest rocks. Dev. Precambrian Geol.* 15, 607–667.
- Nikolaeva, K., Gerya, T.V., Connolly, J.A.D., 2008. Numerical modeling of crustal growth in intraoceanic volcanic arcs. *Phys. Earth Planet. Inter.* 171, 336–356.
- Nutman, A.P., Friend, C.R.L., Baadsgaard, H., McGregor, V.R., 1989. Evolution and assembly of Archean gneiss terranes in the Godthåbsfjord region, southern west Greenland: structural, metamorphic, and isotopic evidence. *Tectonics* 8, 573–589, <http://dx.doi.org/10.1029/TC0081003p00573>.
- Nutman, A.P., Friend, C.R.L., Horie, K., Hidaka, H., 2007. The Itsaq gneiss complex of southern West Greenland and the construction of Eoarchean crust at convergent plate boundaries. In: Van Kranendonk, M.J., Smithies, R.H., Bennett, V. (Eds.), *Earth's Oldest Rocks: Developments in Precambrian Geology*, 15. Elsevier, Amsterdam, pp. 187–218, [http://dx.doi.org/10.1016/S0166-2635\(07\)15041-6](http://dx.doi.org/10.1016/S0166-2635(07)15041-6).
- Nutman, A.P., Friend, C.R.L., Paxton, S., 2009. Detrital zircon sedimentary provenance ages for the Eoarchean Itsaq Supracrustal Belt southern West Greenland: Juxtaposition of an imbricated ca. 3700 Ma juvenile arc against an older complex with 3920–3760 Ma components. *Tectonophysics* 172, 212–233, <http://dx.doi.org/10.1016/j.tectonophysics.2009.03.019>.
- Nutman, A.P., Bennett, V.C., Friend, C.R.L., Hidaka, H., Yi, K., Lee, S.R., Kamiuchi, T., 2013. The Itsaq gneiss complex of Greenland: episodic 3900 to 3660 ma juvenile crust formation and recycling in the 3660 to 3600 Ma Isukasian orogeny. *Am. J. Sci.* 313, 877–911.
- O'Neill, C., Jellinek, A.M., Lenardic, A., 2007a. Conditions for the onset of plate tectonics on terrestrial planets and moons. *Earth Planet. Sci. Lett.* 261, 20–32.
- O'Neill, C., Lenardic, A., Moresi, L., Torsvik, T., Lee, C.A., 2007b. Episodic Precambrian subduction. *Earth Planet. Sci. Lett.* 262, 552–562.
- O'Neill, C., Debaile, V., 2014. The evolution of Hadean–Eoarchean geodynamics. *Earth Planet. Sci. Lett.* 406, 49–58.
- O'Neill, C., Lenardic, A., Condie, K.C., 2015. Earth's punctuated tectonic evolution: cause and effect. *Geological Society, London, Special Publications* 389, 17–40.
- Park, R.G., 1981. Origin of gorslton structure in high-grade Archean terrains. *Spec. Publ. Ser. Geol. Soc. Aust.* 7, 481–490.
- Pearson, D.G., Wittig, N., 2008. Formation of Archean continental lithosphere and its diamonds: the root of the problem. *J. Geol. Soc. Lond.* 165, 895–914.
- Percival, J.A., Skulski, T., Sanborn-Barrie, M., Stott, G.M., Leclair, A.D., Corkery, M.T., Boily, M., 2012. Geology and tectonic evolution of the Superior Province, Canada. In: Percival, J., Clowes, R., Cook, F.A. (Eds.), *Tectonic Styles in Canada: The Lithoprobe Perspective*. Geological Association of Canada, St. Johns, NL, Canada, pp. 321–378.
- Polat, A., Kerrich, R., 2006. Reading the geochemical fingerprints of Archean hot subduction volcanic rocks: evidence for accretion and crustal recycling in a mobile tectonic regime. In: Benn, K., Mareschal, J.-C., Condie, K.C. (Eds.), *Archean Geodynamics and Environments*. Geophysical Monograph, American Geophysical Union, 164, 189–213.
- Polat, A., Kerrich, R., Wyman, D.A., 1998. The late Archean Schreiber-Hemlo and White River-Dayohessarah greenstone belts, Superior Province: collages of Oceanic plateaus, oceanic arcs, and subduction–accretion complexes. *Tectonophysics* 294, 295–326.
- Polat, A., Kerrich, R., Windley, B., 2009. Archean crustal growth processes in southern West Greenland and the southern Superior Province: geodynamic and magmatic constraints. In: Cawood, P.A., Kröner, A. (Eds.), *Earth Accretionary Systems in Space and Time*. The Geological Society, London, Special Publications, 318, pp. 155–191, <http://dx.doi.org/10.1144/SP318.6>.
- Poli, S., Schmidt, M.W., 2002. Petrology of subducted slabs. *Annu. Rev. Earth Planet. Sci.* 30, 207–235.

- Puchtel, I.S., Hofmann, A.W., Mezger, K., Jochum, K.P., Shchipansky, A.A., Samsonov, A.V., 1998. Oceanic plateau model for continental crustal growth in the Archean: a case study from the Kostomuksha greenstone belt, NWBaltic Shield. *Earth Planet. Sci. Lett.* 155, 57–74.
- Qian, Q., Hermann, J., 2013. Partial melting of lower crust at 10–15 kbar: constraints on adakite and TTG formation. *Contrib. Mineral. Petrol.* 165, 119–1224.
- Ranalli, G., 1995. *Rheology of the Earth*. Chapman and Hall, London, pp. 413.
- Rapp, R.P., Watson, E.B., Miller, C.F., 1991. Partial melting of amphibolite/eclogite and the origin of Archean trondjemites and tonalites. *Precambrian Res.* 51, 1–25.
- Rapp, R.P., Shimizu, N., Norman, M.D., 2003. Growth of early continental crust by partial melting of eclogite. *Nature* 425, 605–609.
- Rapp, R., Norman, M., Laporte, D., Yaxley, G., Martin, H., Foley, S., 2010. Continent formation in the Archean and chemical evolution of the cratonic lithosphere: melt–rock reaction experiments at 3–4 GPa and petrogenesis of Archean Mg-diorites (sanukitoids). *J. Petrol.* 51, 1237.
- Rey, P.F., Coltice, N., Flament, N., 2014. Spreading continents kick-started plate tectonics. *Nature* 513, 405–408. <http://dx.doi.org/10.1038/nature13728>.
- Schenker, F.L., Gerya, T., Burg, J.-P., 2012. Bimodal behavior of extended continental lithosphere: modeling insight and application to thermal history of migmatitic core complexes. *Tectonophysics* 579, 88–103.
- Schmalzl, J., Houseman, G.A., Hansen, U., 1996. Mixing in vigorous, time-dependent three-dimensional convection and application to Earth's mantle. *J. Geophys. Res.* 101, 21847–21858.
- Schmeling, H., 2006. A model of episodic melt extraction for plumes. *J. Geophys. Res.* 111, <http://dx.doi.org/10.1029/2004JB003423>.
- Schmeling, H., Babeyko, A.Y., Enns, A., Faccenna, C., Funiciello, F., Gerya, T., Golabek, G.J., Grigull, S., Kaus, B.J.P., Morra, G., Schmalholz, S.M., van Hunen, J., 2008. Benchmark comparison of spontaneous subduction models—towards a free surface. *Phys. Earth Planet. Inter.* 171 (1–4), 198–223.
- Schmidt, M., Poli, S., 1998. Experimentally based water budgets for dehydrating slabs and consequences for arc magma generation. *Earth Planet. Sci. Lett.* 163, 361–379.
- Sizova, E., Gerya, T., Brown, M., Perchuk, L.L., 2010. Subduction styles in the Precambrian: insight from numerical experiments. *Lithos* 116, 209–229.
- Sizova, E., Gerya, T., Brown, M., 2014. Contrasting styles of Phanerozoic and Precambrian continental collision. *Gondwana Res.* 25 (2), 522–545, <http://dx.doi.org/10.1016/j.gr.2012.12.011>.
- Smithies, R.H., 2000. The Archean tonalite–trondjemite–granodiorite (TTG) series is not an analogue of Cenozoic adakite. *Earth Planet. Sci. Lett.* 182, 115–125.
- Smithies, R.H., Van Kranendonk, M.J., Champion, D.C., 2005. It started with a plume—early Archean basaltic proto-continent crust. *Earth Planet. Sci. Lett.* 238, 284–297, <http://dx.doi.org/10.1016/j.epsl.2005.07.023>.
- Smithies, R.H., Champion, D.C., Van Kranendonk, M.J., 2009. Formation of Paleoproterozoic continental crust through infracrustal melting of enriched basalt. *Earth Planet. Sci. Lett.* 281, 298–306.
- Springer, W., Seck, H.A., 1997. Partial fusion of basic granulites at 5 to 15 kbar: implications for the origin of TTG magmas. *Contrib. Mineral. Petrol.* 127, 30–45.
- Tatsumi, Y., Suzuki, T., Ozawa, H., Hirose, K., Hanyu, T., Ohishi, Y., 2014. Accumulation of “anti-continent” at the base of the mantle and its recycling in mantle plumes. *Geochim. Cosmochim. Acta* 143, 23–33.
- Thébaut, N., Rey, P.F., 2013. Archean gravity-driven tectonics on hot and flooded continents: controls on long-lived mineralised hydrothermal systems away from continental margins. *Precambrian Res.* 229, 93–104.
- Thybo, H., Artemieva, I.M., 2013. Moho and magmatic underplating in continental lithosphere. *Tectonophysics* 609, 605–619.
- Turcotte, D.L., Schubert, G., 2002. *Geodynamics*. Cambridge University Press, pp. 456.
- Van Hunen, J., van den Berg, A.P., 2008. Plate tectonics on the early Earth: limitations imposed by strength and buoyancy of subducted lithosphere. *Lithos* 103, 217–235.
- Van Keken, P.E., Zhong, S.J., 1999. Mixing in a 3D spherical model of present-day mantle convection. *Earth Planet. Sci. Lett.* 171, 533–547.
- Van Kranendonk, M.J., 2010. Two types of Archean continental crust: plume and plate tectonics on early Earth. *Am. J. Sci.* 310, 1187–1209.
- Van Kranendonk, M.J., 2011. Cool greenstone drips and the role of partial convective overturn in Barberton greenstone belt evolution. *J. Afr. Earth Sci.* 60, 346–352.
- Van Kranendonk, M.J., Smithies, R.H., Hickman, A.H., Champion, D.H., 2007. Secular tectonic evolution of Archean continental crust: interplay between horizontal and vertical processes in the formation of the Pilbara Craton, Australia. *Terra Nova* 19, 1–38.
- Van Kranendonk, M.J., Kröner, A., Hegner, E., Connelly, J., 2009. Age, lithology and structural evolution of the c. 3.53 Ga Threespruit formation in the Tjakkastad area, southwestern Barberton Greenstone belt, South Africa, with implications for Archean tectonics. *Chem. Geol.* 261, 114–138.
- Van Kranendonk, M.J., Kröner, A., Hoffman, E.J., Nagel, T., Anhaeusser, C.R., 2014. Just another drip: re-analysis of a proposed Mesoarchean suture from the Barberton Mountain Land, South Africa. *Precambrian Res.* 254, 19–35.
- Van Thienen, P., Van den Berg, A.P., 2004. On the formation of continental silicic melts in thermochemical mantle convection models: implication for early Earth. *Tectonophysics* 394, 111–124.
- Vlaar, N.J., van Keken, P.E., van den Berg, 1994. Cooling of the Earth in the Archean: consequences of pressure release melting in a hotter mantle. *Earth Planet. Sci. Lett.* 121, 1–18.
- Vogt, K., Gerya, T., Castro, A., 2012. Crustal growth at active continental margins: numerical modeling. *Phys. Earth Planet. Inter.* 192–193, 1–20.
- Willbold, M., Hegner, E., Stracke, A., Rocholl, A., 2009. Continental geochemical signatures in dacites from Iceland and implications for models of early Archean crust formation. *Earth Planet. Sci. Lett.* 279, 44–52.
- Windley, B.F., Bridgwater, D., 1971. The evolution of Archean low- and high-grade terrains. *Geological Society of Australia, Special Publication* 3, 33–46.
- Zeh, A., Gerdes, A., Barton, J.M., 2009. Archean accretion and crustal evolution of the Kalahari Craton—the zircon age and Hf isotope record of granitic rocks from Barberton/Swaziland to the Francistown Arc. *J. Petrol.* 50, 933–966, <http://dx.doi.org/10.1093/petrology/egp027>.
- Zeh, A., Jaguin, J., Poujol, M., Boulvais, P., Block, S., Paquette, J.L., 2013. Juvenile crust formation in the northeastern Kaapvaal Craton at 2.97 Ga—implications for Archean terrane accretion, and the source of the Pietersburg gold. *Precambrian Res.* 233, 20–43.
- Zhang, C., Holtz, F., Koepke, J., Wolff, P.E., Ma, C., Bedard, J.H., 2013. Constraints from experimental melting of amphibolite on the depth of formation of garnet-rich restites, and implications for models of Early Archean crustal growth. *Precambrian Res.* 231, 206–217.